Contemporary Mathematics

Analysis and Efficient Computation for the Dynamics of Two-Component Bose-Einstein Condensates

Weizhu Bao

Abstract. In this paper, we review some recent results on the analysis and efficient computation for the dynamics of rotating two-component Bose-Einstein condensates (BECs). We begin with the three-dimensional (3D) coupled Gross-Pitaevskii equations (GPEs) with an angular momentum rotation term and an external driving field, show how to scale it into dimensionless form, reduce it to a 2D and 1D GPE in the limiting regime of strong anisotropic confinement and present its semiclassical scaling and geometric optics. Dynamic laws on the angular momentum expectation, density of each component, condensate widths and analytical solutions of stationary states with its center shifted from the trapping center are presented. In addition, efficient and accurate numerical methods for computing the dynamics of rotating two-component BEC are presented and some numerical results are reported to demonstrate the efficiency and accuracy of the numerical methods.

1. Introduction

This paper summarizes recent work by the author on analysis and efficient computation for the dynamics of rotating two-component Bose-Einstein condensate (BEC) with/without an external driving field [**2, 19, 14**]. Although the theories and numerical methods presented here apply to multi-component BEC with any number of components [**43, 40, 1, 28, 30**], we concentrate here on two-component BEC for simplicity [**28, 29, 42, 33**]. At temperatures T much smaller than the critical temperature T_c [**44, 20**], in the rotating frame, a two-component BEC with an external driving field can be well described by two self-consistent nonlinear Schrödinger equations (NLSEs), also known as coupled Gross-Pitaevskii equations (CGPEs) [**32, 22, 37, 36**],

(1.1)
$$i\hbar\frac{\partial\psi_j(\mathbf{x},t)}{\partial t} = \left[-\frac{\hbar^2}{2m}\nabla^2 + \hbar\kappa_j + V_j(\mathbf{x}) - \Omega L_z + \sum_{l=1}^{2} U_{jl}|\psi_l|^2\right]\psi_j - \lambda\hbar\psi_{k_j},\ j=1,2,$$

Key words and phrases. Bose-Einstein condensation, two-component, ground state, dynamics, external driving field, condensate width, time-splitting.

The author acknowledges support from the Ministry of Education of Singapore grant No. R-146-000-083-112.

where $\psi_j(\mathbf{x},t)$ denotes the macroscopic wave function of the jth ($j=1,2$) component with $\mathbf{x}=(x,y,z)^T$ being the Cartesian coordinate vector and t being time, $\hbar$ is the Planck constant, m is the atomic mass (for simplicity, here we assume that the atomic mass of the two components is the same), Ω is the angular velocity of the rotating laser beam, $L_z=-i\hbar(x\partial_y-y\partial_x)$ is the z-component of the angular momentum, κ_j ($j=1,2$) are the Raman transition constants [**30**], and λ is the effective Rabi frequency describing the strength of the external driving field. $V_j(\mathbf{x})$ is the external trapping potential acting on the jth component, and if the harmonic potential is considered, it takes the form

$$V_j(\mathbf{x})=\frac{m}{2}\left(\omega_{x,j}^2\,x^2+\omega_{y,j}^2\,y^2+\omega_{z,j}^2\,z^2\right),\qquad j=1,2, \tag{1.2}$$

with $\omega_{x,j}$, $\omega_{y,j}$ and $\omega_{z,j}$ the trapping frequencies of the jth component in x-, y- and z-directions, respectively. The interactions of particles are described by $U_{jl}=4\pi\hbar^2a_{jl}/m$ with $a_{jl}=a_{lj}$ ($j,l=1,2$) being the s-wave scattering lengths between the jth and lth component (positive for repulsive interaction and negative for attractive interaction). The integers k_j in (1.1) are chosen as

$$k_j=\begin{cases}2, & j=1,\\ 1, & j=2.\end{cases} \tag{1.3}$$

It is necessary to ensure that the wave functions are properly normalized. Especially, we require

$$\int_{\mathbb{R}^3}\left(|\psi_1(\mathbf{x},t)|^2+|\psi_2(\mathbf{x},t)|^2\right)d\mathbf{x}=N=N_1^0+N_2^0,\qquad t\geq 0, \tag{1.4}$$

where

$$N_j^0=\int_{\mathbb{R}^3}|\psi_j(\mathbf{x},0)|^2\,d\mathbf{x}, \tag{1.5}$$

is the particle number of the jth ($j=1,2$) component at time $t=0$ and N is the total number of particles in the condensate.

Under the normalization (1.4), we introduce the dimensionless variables as follows: $t\to t/\omega_m$ with $\omega_m=\min_{1\leq j\leq 2}\{\omega_{x,j},\omega_{y,j},\omega_{z,j}\}$, $\Omega\to\omega_m\,\Omega$, $\kappa_j\to\omega_m\,\kappa_j$, $\lambda\to\omega_m\,\lambda$, $\mathbf{x}\to a_0\mathbf{x}$ with $a_0=\sqrt{\hbar/m\omega_m}$, and $\psi_j\to\psi_j\sqrt{N}/a_0^{3/2}$, i.e. we choose $1/\omega_m$ and a_0 as the dimensionless time unit and length unit, respectively. After some computations from (1.1), we obtain the dimensionless CGPEs as

$$i\frac{\partial\psi_j(\mathbf{x},t)}{\partial t}=\left[-\frac{1}{2}\nabla^2+\kappa_j+V_j(\mathbf{x})-\Omega L_z+\sum_{l=1}^{2}\beta_{jl}|\psi_l|^2\right]\psi_j-\lambda\psi_{k_j},\ j=1,2, \tag{1.6}$$

where the dimensionless interaction parameters are characterized by $\beta_{jl}=\beta_{lj}=\frac{mU_{jl}N}{\hbar^2a_0}=\frac{4\pi Na_{jl}}{a_0}$ ($j,l=1,2$). The dimensionless angular momentum rotation term becomes

$$L_z=-i(x\partial_y-y\partial_x)=-i\,\partial_\theta:=-i\,\widehat{L}_z \tag{1.7}$$

with (r,θ) the polar coordinate in 2D, and resp. (r,θ,z) the cylindrical coordinate in 3D. The dimensionless external potentials are

$$V_j(\mathbf{x})=\frac{1}{2}\left(\gamma_{x,j}^2\,x^2+\gamma_{y,j}^2\,y^2+\gamma_{z,j}^2\,z^2\right),\qquad j=1,2 \tag{1.8}$$

with $\gamma_{x,j}=\omega_{x,j}/\omega_m$, $\gamma_{y,j}=\omega_{y,j}/\omega_m$ and $\gamma_{z,j}=\omega_{z,j}/\omega_m$ ($j=1,2$).

Theoretical treatment of such systems began in the context of superfluid helium mixtures and spin polarized hydrogen, and has now been extended to BEC in alkalis [**29, 20, 35, 45**]. With the realization of BEC in experiments, the theoretical predications of multi-component condensates, e.g. density profile, dynamics of interacting BEC [**26**], motion damping [**30**] and formation of vortices, can now be compared with experimental data [**28, 3**]. Needless to say that this dramatic progress on the experimental front has stimulated a wave of activity on both theoretical and numerical fronts.

The paper is organized as follows. In section 2, we review dimension reduction and geometric optics of coupled GPEs. In section 3, we review the dynamic laws for the density of each component, angular momentum expectation, condensate width and a stationary state with its center shifted from the trap center. In section 4, we review efficient and accurate numerical methods for computing the dynamics of two-component BEC. In section 5, some numerical results are reported. Finally, some conclusions are drawn in section 6.

2. The coupled Gross-Pitaevskii equations

In this section, we will review dimension reduction of the coupled GPEs, reduction to one-component BEC, and the semiclassical scaling and geometric optics in strongly repulsive interaction regimes.

2.1. Dimension reduction. In a disk-shaped condensate, i.e.

$$\omega_{x,j} \approx \omega_{y,j} \approx \omega_m, \quad \omega_{z,j} \gg \omega_m \iff \gamma_{x,j} \approx \gamma_{y,j} \approx 1, \quad \gamma_{z,j} \gg 1, \quad j = 1, 2,$$

the 3D CGPEs (1.6) can be formally reduced to 2D CGPEs with $\mathbf{x} = (x, y)^T$ [**41, 7, 5, 6**]. When $\Omega = 0$ and in a cigar-shaped condensate, i.e.

$$\omega_{x,j} \approx \omega_m,\ \omega_{y,j} \gg \omega_m,\ \omega_{z,j} \gg \omega_m \Longleftrightarrow \gamma_{x,j} \approx 1,\ \gamma_{y,j} \gg 1,\ \gamma_{z,j} \gg 1,\ j = 1, 2,$$

the 3D CGPEs (1.6) can be formally reduced to 1D CGPEs with $\mathbf{x} = x$ [**41, 7, 5, 6**]. Thus here we consider the following CGPEs in d-dimensions ($d = 2, 3$ when $\Omega \neq 0$ and $d = 1, 2, 3$ when $\Omega = 0$):

$$i\frac{\partial \psi_j(\mathbf{x}, t)}{\partial t} = \left[-\frac{1}{2}\nabla^2 + \kappa_j + V_j(\mathbf{x}) - \Omega L_z + \sum_{l=1}^{2} \beta_{j\,l} |\psi_l|^2\right] \psi_j - \lambda \psi_{k_j},\ t \geq 0, \tag{2.1}$$

$$\psi_j(\mathbf{x}, 0) = \psi_j^0(\mathbf{x}), \qquad \mathbf{x} \in \mathbb{R}^d, \tag{2.2}$$

where the initial data are normalized as

$$\|\psi_1^0\|^2 + \|\psi_2^0\|^2 := \int_{\mathbb{R}^d} \left(|\psi_1^0(\mathbf{x})|^2 + |\psi_2^0(\mathbf{x})|^2\right) d\mathbf{x} = \frac{N_1^0}{N} + \frac{N_2^0}{N} = 1, \tag{2.3}$$

and the external potentials are given as

$$V_j(\mathbf{x}) = \begin{cases} \frac{1}{2}\gamma_{x,j}^2\, x^2, & d = 1, \\ \frac{1}{2}\left(\gamma_{x,j}^2\, x^2 + \gamma_{y,j}^2\, y^2\right), & d = 2, \\ \frac{1}{2}\left(\gamma_{x,j}^2\, x^2 + \gamma_{y,j}^2\, y^2 + \gamma_{z,j}^2\, z^2\right), & d = 3, \end{cases} \qquad j = 1, 2. \tag{2.4}$$

In fact, in (2.1), if $\Omega = 0$, then the equations are for nonrotating two-component BEC, and if $\Omega \neq 0$, they are for rotating two-component BEC; if $\lambda = 0$, there is no external driving field, and if $\lambda \neq 0$, there is an external driving field.

The dimensionless CGPEs (2.1) conserve the total density:

$$N(t) = N_1(t) + N_2(t) \equiv \|\psi_1^0\|^2 + \|\psi_2^0\|^2 = 1, \qquad t \geq 0 \tag{2.5}$$

with

$$N_j(t) = \|\psi_j(\cdot,t)\|^2 := \int_{\mathbb{R}^d} |\psi_j(\mathbf{x},t)|^2 \, d\mathbf{x}, \qquad t \geq 0, \quad j = 1,2, \tag{2.6}$$

and the energy

$$\begin{aligned} E(\psi_1,\psi_2) &= \int_{\mathbb{R}^d} \left[\sum_{j=1}^{2} \left(\frac{1}{2}|\nabla\psi_j|^2 + (\kappa_j + V_j(\mathbf{x}))\,|\psi_j|^2 - \Omega\ \mathrm{Re}\left(\psi_j^* L_z \psi_j\right) \right.\right. \\ &\qquad \left.\left. + \sum_{l=1}^{2} \frac{\beta_{jl}}{2}|\psi_j|^2|\psi_l|^2 \right) - 2\lambda\ \mathrm{Re}(\psi_1^*\psi_2) \right] d\mathbf{x} \\ &\equiv E\left(\psi_1^0,\psi_2^0\right), \qquad t \geq 0 \end{aligned} \tag{2.7}$$

with f^* and $\mathrm{Re}(f)$ denoting the conjugate and real part of a function f, respectively. In addition, if there is no external driving field in (2.1), i.e. $\lambda = 0$, the density of each component is also conserved, i.e.

$$N_j(t) = \int_{\mathbb{R}^d} |\psi_j(\mathbf{x},t)|^2 \ d\mathbf{x} \equiv \|\psi_j^0\|^2 = \frac{N_j^0}{N}, \qquad t \geq 0, \quad j = 1,2. \tag{2.8}$$

2.2. Reduction to single GPE. If there is no external driving field in (2.1), i.e. $\lambda = 0$, and the initial particle numbers of the two components N_1^0 and N_2^0 (w.l.o.g., assuming that $N_1^0 \geq N_2^0$) in (1.4) satisfy $N_1^0 \gg N_2^0$, i.e. $N_1^0 = O(N)$ and $N_2^0 = o(N)$, when $N \gg 1$, we have

$$N_2(t) = \int_{\mathbb{R}^d} |\psi_2(\mathbf{x},t)|^2 \, d\mathbf{x} \equiv \frac{N_2^0}{N} := \varepsilon \ll 1, \tag{2.9}$$

$$N_1(t) = \int_{\mathbb{R}^d} |\psi_1(\mathbf{x},t)|^2 \, d\mathbf{x} \equiv \frac{N_1^0}{N} := 1 - \varepsilon \approx 1, \qquad t \geq 0. \tag{2.10}$$

These immediately imply that the effect of the second component is insignificant and the original two-component system is mainly dominated by the first component. Formally, we can drop the second component from the two-component BEC and get a single-component BEC, and in this case the CGPEs (2.1) are reduced to

$$i\frac{\partial\psi(\mathbf{x},t)}{\partial t} = \left[-\frac{1}{2}\nabla^2 + \kappa + V(\mathbf{x}) + \beta|\psi|^2 - \Omega L_z \right] \psi, \qquad t \geq 0 \tag{2.11}$$

by setting $\psi(\mathbf{x},t) = \sqrt{N/N_1^0}\,\psi_1(\mathbf{x},t)$, $\kappa = \kappa_1$, $V(\mathbf{x}) = V_1(\mathbf{x})$ and $\beta = N_1^0\beta_{11}/N \approx \beta_{11}$. The GPE (2.11) conserves the normalization of the wave function

$$\|\psi(\cdot,t)\|^2 \equiv \int_{\mathbb{R}^d} |\psi(\mathbf{x},0)|^2 \, d\mathbf{x} = \int_{\mathbb{R}^d} \frac{N}{N_1^0}|\psi_1(\mathbf{x},0)|^2 \, d\mathbf{x} = \frac{N}{N_1^0}\frac{N_1^0}{N} = 1, \ t \geq 0, \tag{2.12}$$

and the energy

$$E_s(\psi) = \int_{\mathbb{R}^d} \left[\frac{1}{2}\,|\nabla\psi|^2 + (\kappa + V(\mathbf{x}))\,|\psi|^2 - \Omega\ \mathrm{Re}\,(\psi^* L_z\psi) + \frac{\beta}{2}|\psi|^4 \right] d\mathbf{x}, \ t \geq 0. \tag{2.13}$$

In addition, by setting $\psi_1(\mathbf{x},t)=\sqrt{N_1^0/N}\psi(\mathbf{x},t)$ and $\psi_2(\mathbf{x},t)=\sqrt{N_2^0/N}\phi(\mathbf{x},t)$ in the energy of the two-component BEC (2.7) with $\lambda=0$, we obtain

$$\begin{aligned} E(\psi_1,\psi_2) &= \frac{N_1^0}{N}E_s(\psi)+\frac{N_2^0}{N}E_r(\psi,\phi)=(1-\varepsilon)E_s(\psi)+\varepsilon\, E_r(\psi,\phi) \\ &= E_s(\psi)+\varepsilon\left[-E_s(\psi)+E_r(\psi,\phi)\right], \end{aligned} \tag{2.14}$$

where

$$\begin{aligned} E_r(\psi,\phi) &= \int_{\mathbb{R}^d}\left[\frac{1}{2}\left|\nabla\phi\right|^2+\kappa_2|\phi|^2+V_2(\mathbf{x})|\phi|^2-\Omega\,\mathrm{Re}\left(\phi^*L_z\phi\right)\right. \\ &\quad \left.+\beta_{21}\frac{N_1^0}{N}|\psi|^2|\phi|^2+\frac{\beta_{22}}{2}\frac{N_2^0}{N}|\phi|^4\right]d\mathbf{x}. \end{aligned} \tag{2.15}$$

This formally implies that the relative error between the energy of the two-component BEC (2.7) and that of the single-component BEC (2.13) converges to 0 linearly when $\varepsilon=\frac{N_2^0}{N}$ goes to 0, i.e.

$$\frac{|E(\psi_1,\psi_2)-E_s(\psi)|}{E_s(\psi)}=\varepsilon\left[1-\frac{E_r(\psi,\phi)}{E_s(\psi)}\right]=O(\varepsilon),\quad \text{when}\quad 0<\varepsilon\ll 1. \tag{2.16}$$

2.3. Semiclassical scaling and leading asymptotics in energy. Let $\beta_{\max}=\max\{\beta_{11},\beta_{12},\beta_{22}\}$. If $\beta_{\max}\gg 1$, i.e. in the strong repulsive interaction regime or there are many particles in the condensate, under the normalization (2.5), the semiclassical scaling for the CGPEs (2.1) is also very useful in practice by choosing

$$\mathbf{x}=\varepsilon^{-1/2}\mathbf{x},\qquad \psi_j^\varepsilon=\varepsilon^{d/4}\psi_j,\qquad \varepsilon=\beta_{\max}^{-2/(d+2)}. \tag{2.17}$$

Substituting (2.17) into (2.1), we get the CGPEs in the semiclassical scaling under the normalization (2.5) with $\psi_j=\psi_j^\varepsilon$ $(j=1,2)$:

$$i\varepsilon\frac{\partial\psi_j^\varepsilon(\mathbf{x},t)}{\partial t}=\left[-\frac{\varepsilon^2}{2}\nabla^2+\varepsilon\kappa_j+V_j(\mathbf{x})-\varepsilon\Omega L_z+\sum_{l=1}^{2}\alpha_{jl}\left|\psi_l^\varepsilon\right|^2\right]\psi_j^\varepsilon-\varepsilon\lambda\psi_{k_j}^\varepsilon,\ j=1,2, \tag{2.18}$$

where $\alpha_{jl}=\beta_{jl}/\beta_{\max}=O(1)$ (or $o(1)$). In this case, the associated energy functional $E^\varepsilon(\psi_1^\varepsilon,\psi_2^\varepsilon)$ is defined as

$$\begin{aligned} E^\varepsilon\left(\psi_1^\varepsilon,\psi_2^\varepsilon\right) &= \int_{\mathbb{R}^d}\left[\sum_{j=1}^{2}\left(\frac{\varepsilon^2}{2}|\nabla\psi_j^\varepsilon|^2+\left(\varepsilon\kappa_j+V_j(\mathbf{x})\right)|\psi_j^\varepsilon|^2-\varepsilon\Omega\,\mathrm{Re}\left((\psi_j^\varepsilon)^*L_z\psi_j^\varepsilon\right)\right.\right. \\ &\quad \left.\left.+\sum_{l=1}^{2}\frac{\alpha_{jl}}{2}|\psi_j^\varepsilon|^2|\psi_l^\varepsilon|^2\right)-2\varepsilon\lambda\,\mathrm{Re}\left((\psi_1^\varepsilon)^*\psi_2^\varepsilon\right)\right]d\mathbf{x}=O(1),\ \ t\geq 0, \end{aligned} \tag{2.19}$$

by assuming that ψ_j^ε is ε-oscillatory (see (2.21)) and 'sufficiently' integrable such that all terms have $O(1)$-integral. Then the leading asymptotics of the energy functional $E(\psi_1,\psi_2)$ in (2.7) can be given by

$$E(\psi_1,\psi_2)=\varepsilon^{-1}E^\varepsilon(\psi_1^\varepsilon,\psi_2^\varepsilon)=O(\varepsilon^{-1})=O\left(\beta_{\max}^{2/(d+2)}\right). \tag{2.20}$$

2.4. Geometrical optics of nonrotating two-component BEC. For nonrotating two-component BEC without external driving field and in strongly repulsive interaction regimes, i.e. $\Omega = 0$, $\lambda = 0$ and $0 < \varepsilon \ll 1$ in (2.18), we can set, i.e. the WKB ansatz [**24**]

$$\psi_j^\varepsilon(\mathbf{x},t) = \sqrt{\rho_j^\varepsilon(\mathbf{x},t)}\exp\left(\frac{i}{\varepsilon}S_j^\varepsilon(\mathbf{x},t)\right), \qquad j=1,2, \tag{2.21}$$

where $\rho_j^\varepsilon = |\psi_j^\varepsilon|^2$ and $S_j^\varepsilon = \varepsilon \arg\left(\psi_j^\varepsilon\right)$ are the position density and phase of the wave function ψ_j^ε of jth-component ($j=1,2$), respectively. Inserting (2.21) into (2.18) and collecting the real and imaginary parts, we get the coupled transport equations for the densities ρ_j^ε and the Hamilton-Jacobi equations for the phases S_j^ε ($j=1,2$):

$$\partial_t \rho_j^\varepsilon + \mathrm{div}\left(\rho_j^\varepsilon \nabla S_j^\varepsilon\right) = 0, \tag{2.22}$$

$$\partial_t S_j^\varepsilon + \frac{1}{2}|\nabla S_j^\varepsilon|^2 + \varepsilon\kappa_j + V_j(\mathbf{x}) + \sum_{l=1}^{2}\alpha_{jl}\rho_l^\varepsilon = \frac{\varepsilon^2}{2\sqrt{\rho_j^\varepsilon}}\nabla^2\sqrt{\rho_j^\varepsilon}, \quad j=1,2. \tag{2.23}$$

Furthermore, by defining the current densities

$$\mathbf{J}_j^\varepsilon(\mathbf{x},t) = \rho_j^\varepsilon \nabla S_j^\varepsilon = \varepsilon\,\mathrm{Im}\left[\left(\psi_j^\varepsilon\right)^*\nabla\psi_j^\varepsilon\right], \qquad j=1,2, \tag{2.24}$$

where $\mathrm{Im}(f)$ is the imaginary part of a function f, we can rewrite (2.22)-(2.23) as a coupled Euler system with third-order dispersion terms

$$\partial_t \rho_j^\varepsilon + \mathrm{div}\mathbf{J}_j^\varepsilon = 0, \qquad j=1,2, \tag{2.25}$$

$$\partial_t \mathbf{J}_j^\varepsilon + \mathrm{div}\left(\frac{\mathbf{J}_j^\varepsilon\otimes\mathbf{J}_j^\varepsilon}{\rho_j^\varepsilon}\right) + \rho_j^\varepsilon\nabla V_j(\mathbf{x}) + \nabla P_j\left(\rho_1^\varepsilon,\rho_2^\varepsilon\right) = \frac{\varepsilon^2}{4}\nabla\left(\rho_j^\varepsilon\nabla^2\ln\rho_j^\varepsilon\right); \tag{2.26}$$

where the pressures P_j are defined as

$$P_j\left(\rho_1^\varepsilon,\rho_2^\varepsilon\right) = \frac{1}{2}\sum_{l=1}^{2}\alpha_{jl}\,\rho_j^\varepsilon\,\rho_l^\varepsilon, \qquad j=1,2.$$

By formally passing to the limit $\varepsilon\to 0^+$ in (2.22)-(2.23), we get

$$\partial_t \rho_j^0 + \mathrm{div}\left(\rho_j^0\nabla S_j^0\right) = 0, \tag{2.27}$$

$$\partial_t S_j^0 + \frac{1}{2}|\nabla S_j^0|^2 + V_j(\mathbf{x}) + \sum_{l=1}^{2}\alpha_{jl}\rho_l^0 = 0, \qquad j=1,2, \tag{2.28}$$

with $\rho_j^0 = \lim_{\varepsilon\to 0^+}\rho_j^\varepsilon$ and $S_j^0 = \lim_{\varepsilon\to 0^+} S_j^\varepsilon$. Similarly, letting $\varepsilon\to 0^+$ in (2.25)-(2.26), formally we get an Euler system coupling through the pressures

$$\partial_t \rho_j^0 + \mathrm{div}\mathbf{J}_j^0 = 0, \qquad j=1,2, \tag{2.29}$$

$$\partial_t \mathbf{J}_j^0 + \mathrm{div}\left(\frac{\mathbf{J}_j^0\otimes\mathbf{J}_j^0}{\rho_j^\varepsilon}\right) + \rho_j^0\nabla V_j(\mathbf{x}) + \nabla P_j\left(\rho_1^0,\rho_2^0\right) = 0, \tag{2.30}$$

where $\mathbf{J}_j^0(\mathbf{x},t) = \rho_j^0\nabla S_j^0$ ($j=1,2$). The system (2.29)-(2.30) is a coupled isotropic Euler system with quadratic pressure-density constitutive relations in the nonrotational frame. The formal asymptotics is supposed to hold up to caustic onset time [**24, 25**].

REMARK 2.1. When $\Omega = 0$ and $\lambda \neq 0$ in (2.18), the WKB analysis for studying the semiclassical limit of the nonlinear Schrödinger equation [**24**] is no longer valid for (2.18). Alternatively, one may need to use the Wigner transform [**25**] to study the semiclassical limit of (2.18) when $\lambda \neq 0$.

2.5. Geometrical optics of rotating BEC. For rotating two-component BEC without external driving field and in strongly repulsive interaction regimes, i.e. $\lambda = 0$ and $0 < \varepsilon \ll 1$ in (2.18), due to the appearance of vortices in the initial data (2.2), we set [**27, 15**]

$$\psi_j^\varepsilon(\mathbf{x},t) = \mathbf{A}_j^\varepsilon(\mathbf{x},t)\exp\left(\frac{i}{\varepsilon}S_j^\varepsilon(\mathbf{x},t)\right), \qquad j=1,2, \tag{2.31}$$

where $\mathbf{A}_j^\varepsilon = (a_j^\varepsilon, b_j^\varepsilon) \in \mathbb{C}$ (with $a_j \in \mathbb{R}$ and $b_j \in \mathbb{R}$) represents the density and slow varying phase, and $S_j^\varepsilon = \varepsilon \arg\left(\psi_j^\varepsilon\right)$ is the fast varying phase of the wave function ψ_j^ε of jth-component ($j = 1, 2$). Inserting (2.31) into (2.18) and collecting the $O(1)$ and $O(\varepsilon)$ terms, we get the coupled Schrödinger-type equation for $\mathbf{A}_j^\varepsilon$ and the Hamilton-Jacobi equations for the phases S_j^ε ($j = 1, 2$):

$$\partial_t \mathbf{A}_j^\varepsilon + \nabla S_j^\varepsilon \cdot \nabla \mathbf{A}_j^\varepsilon + \frac{1}{2}\mathbf{A}_j^\varepsilon \Delta S_j^\varepsilon - \Omega\, \widehat{L}_z \mathbf{A}_j^\varepsilon + i\kappa_j \mathbf{A}_j^\varepsilon = \frac{i\varepsilon}{2}\Delta \mathbf{A}_j, \tag{2.32}$$

$$\partial_t S_j^\varepsilon + \frac{1}{2}|\nabla S_j^\varepsilon|^2 + V_j(\mathbf{x}) + \sum_{l=1}^{2}\alpha_{jl}\,|\mathbf{A}_l^\varepsilon|^2 - \Omega\, \widehat{L}_z S_j^\varepsilon = 0, \qquad j=1,2. \tag{2.33}$$

Furthermore, by defining the quantum hydrodynamic velocity

$$\mathbf{u}_j^\varepsilon(\mathbf{x},t) = \nabla S_j^\varepsilon = \varepsilon\,\mathrm{Im}\left[\left(\psi_j^\varepsilon\right)^* \nabla \psi_j^\varepsilon\right]/|\psi_j^\varepsilon|^2, \qquad j=1,2, \tag{2.34}$$

we can rewrite (2.32)-(2.33) as

$$\partial_t \mathbf{A}_j^\varepsilon + \mathbf{u}_j^\varepsilon \cdot \nabla \mathbf{A}_j^\varepsilon + \frac{1}{2}\mathbf{A}_j^\varepsilon \nabla \cdot \mathbf{u}_j^\varepsilon - \Omega\, \widehat{L}_z \mathbf{A}_j^\varepsilon + i\kappa_j \mathbf{A}_j^\varepsilon = \frac{i\varepsilon}{2}\Delta \mathbf{A}_j, \tag{2.35}$$

$$\partial_t \mathbf{u}_j^\varepsilon + (\mathbf{u}_j^\varepsilon \cdot \nabla)\mathbf{u}_j^\varepsilon + \nabla V_j(\mathbf{x}) + \sum_{l=1}^{2}\alpha_{jl}\nabla\,|\mathbf{A}_l^\varepsilon|^2 - \Omega\, \widehat{L}_z \mathbf{u}_j^\varepsilon = 0, \quad j=1,2. \tag{2.36}$$

By formally passing to the limit $\varepsilon \to 0^+$ in (2.32)-(2.33), we get

$$\partial_t \mathbf{A}_j^0 + \nabla S_j^0 \cdot \nabla \mathbf{A}_j^0 + \frac{1}{2}\mathbf{A}_j^0 \Delta S_j^0 - \Omega\, \widehat{L}_z \mathbf{A}_j^0 + i\kappa_j \mathbf{A}_j^0 = 0, \tag{2.37}$$

$$\partial_t S_j^0 + \frac{1}{2}|\nabla S_j^0|^2 + V_j(\mathbf{x}) + \sum_{l=1}^{2}\alpha_{jl}\left|\mathbf{A}_l^0\right|^2 - \Omega\, \widehat{L}_z S_j^0 = 0, \qquad j=1,2; \tag{2.38}$$

where $\mathbf{A}_j^0 = \lim_{\varepsilon\to 0^+}\mathbf{A}_j^\varepsilon$ and $S_j^0 = \lim_{\varepsilon\to 0^+} S_j^\varepsilon$ for $j = 1, 2$. Similarly, letting $\varepsilon \to 0^+$ in (2.35)-(2.36), formally we get

$$\partial_t \mathbf{A}_j^0 + \mathbf{u}_j^0 \cdot \nabla \mathbf{A}_j^0 + \frac{1}{2}\mathbf{A}_j^0 \nabla \cdot \mathbf{u}_j^0 - \Omega\, \widehat{L}_z \mathbf{A}_j^0 + i\kappa_j \mathbf{A}_j^0 = 0, \tag{2.39}$$

$$\partial_t \mathbf{u}_j^0 + (\mathbf{u}_j^0 \cdot \nabla)\mathbf{u}_j^0 + \nabla V_j(\mathbf{x}) + \sum_{l=1}^{2}\alpha_{jl}\nabla\left|\mathbf{A}_l^0\right|^2 - \Omega\, \widehat{L}_z \mathbf{u}_j^0 = 0, \quad j=1,2; \tag{2.40}$$

where $\mathbf{u}_j^0 = \lim_{\varepsilon\to 0^+}\mathbf{u}_j^\varepsilon$ for $j = 1, 2$. The formal asymptotics is supposed to hold up to caustic onset time [**27, 15**].

REMARK 2.2. Again, when $\lambda \neq 0$ and $\Omega \neq 0$ in (2.18), the above formal analysis for studying the semiclassical limit of the nonlinear Schrödinger equation [**27, 15**] is no longer valid for (2.18) with $\Omega \neq 0$. Alternatively, one may need to use the Wigner transform [**25**] to study the semiclassical limit of (2.18) when $\lambda \neq 0$.

3. Dynamics of two-component BEC

In this section, we review the dynamic laws of two-component BEC with external driving field including the conservation of the angular momentum expectation in symmetric traps, time evolution of the density of each component and condensate widths, and analytical solutions for a stationary state with its center shifted from the trap center in rotating two-component BEC.

3.1. Dynamics of the density of each component.

We define

$$W_1(t) = i \int_{\mathbb{R}^d} \left[\psi_1^*(\mathbf{x},t)\psi_2(\mathbf{x},t) - \psi_1(\mathbf{x},t)\psi_2^*(\mathbf{x},t)\right] d\mathbf{x}, \tag{3.1}$$

$$W_2(t) = \int_{\mathbb{R}^d} \left[\psi_1(\mathbf{x},t)\psi_2^*(\mathbf{x},t) + \psi_1^*(\mathbf{x},t)\psi_2(\mathbf{x},t)\right] d\mathbf{x}, \qquad t \geq 0. \tag{3.2}$$

For the dynamics of the density of each component, we have the following lemmas

LEMMA 3.1. *Suppose $(\psi_1(\mathbf{x},t), \psi_2(\mathbf{x},t))$ is the solution of the CGPEs (2.1)-(2.2); then we have,*

$$N_1'(t) - \lambda\, W_1(t) = 0, \qquad N_2'(t) + \lambda\, W_1(t) = 0, \tag{3.3}$$

$$W_1'(t) - 2\lambda\,[1 - 2N_1(t)] + (\kappa_1 - \kappa_2)W_2(t) = F_1(t), \qquad t > 0, \tag{3.4}$$

$$W_2'(t) + (\kappa_2 - \kappa_1)W_1(t) = F_2(t), \tag{3.5}$$

with initial conditions

$$N_1(0) = \int_{\mathbb{R}^d} |\psi_1^0(\mathbf{x})|^2\, d\mathbf{x} = \frac{N_1^0}{N} := N_1^{(0)}, \tag{3.6}$$

$$N_2(0) = \int_{\mathbb{R}^d} |\psi_2^0(\mathbf{x})|^2\, d\mathbf{x} = \frac{N_2^0}{N} := N_2^{(0)}, \tag{3.7}$$

$$W_1(0) = i \int_{\mathbb{R}^d} \left[\left(\psi_1^0\right)^*(\mathbf{x})\psi_2^0(\mathbf{x}) - \psi_1^0(\mathbf{x})\left(\psi_2^0\right)^*(\mathbf{x})\right] d\mathbf{x} := W_1^{(0)}, \tag{3.8}$$

$$W_2(0) = \int_{\mathbb{R}^d} \left[\psi_1^0(\mathbf{x})\left(\psi_2^0\right)^*(\mathbf{x}) + \left(\psi_1^0\right)^*(\mathbf{x})\psi_2^0(\mathbf{x})\right] d\mathbf{x} := W_2^{(0)}; \tag{3.9}$$

where for $t \geq 0$,

$$\begin{aligned} F_1(t) &= \int_{\mathbb{R}^d} (\psi_1^*\psi_2 + \psi_1\psi_2^*)\left[V_2(\mathbf{x}) - V_1(\mathbf{x}) + (\beta_{12} - \beta_{11})|\psi_1|^2\right. \\ &\quad \left. + (\beta_{22} - \beta_{12})|\psi_2|^2\right] d\mathbf{x}, \end{aligned} \tag{3.10}$$

$$\begin{aligned} F_2(t) &= i\int_{\mathbb{R}^d} (\psi_1^*\psi_2 - \psi_1\psi_2^*)\left[V_1(\mathbf{x}) - V_2(\mathbf{x}) + (\beta_{11} - \beta_{12})|\psi_1|^2\right. \\ &\quad \left. + (\beta_{12} - \beta_{22})|\psi_2|^2\right] d\mathbf{x}. \end{aligned} \tag{3.11}$$

Proof. Differentiating (2.6) with respect to t, noticing (2.1), integrating by parts, we obtain

$$\begin{aligned}
N_j'(t) &= \frac{d}{dt}\,\|\psi_j(\cdot,t)\|^2 = \frac{d}{dt}\int_{\mathbb{R}^d}|\psi_j(\mathbf{x},t)|^2\,d\mathbf{x} = \int_{\mathbb{R}^d}\left(\psi_j\partial_t\psi_j^* + \psi_j^*\partial_t\psi_j\right)\,d\mathbf{x}\\
&= i\int_{\mathbb{R}^d}\left[\psi_j\left(\left(-\frac{1}{2}\nabla^2+\kappa_j+V_j(\mathbf{x})-\Omega L_z^*+\sum_{l=1}^{2}\beta_{j\,l}|\psi_l|^2\right)\psi_j^*-\lambda\,\psi_{k_j}^*\right)\right.\\
&\quad\left.-\psi_j^*\left(\left(-\frac{1}{2}\nabla^2+\kappa_j+V_j(\mathbf{x})-\Omega L_z+\sum_{l=1}^{2}\beta_{j\,l}|\psi_l|^2\right)\psi_j-\lambda\,\psi_{k_j}\right)\right]d\mathbf{x}\\
&= i\int_{\mathbb{R}^d}\left[\left(\frac{1}{2}|\nabla\psi_j|^2+(\kappa_j+V_j(\mathbf{x}))\,|\psi_j|^2-\psi_j^*\Omega L_z\psi_j+|\psi_j|^2\sum_{l=1}^{2}\beta_{j\,l}|\psi_l|^2\right)\right.\\
&\quad-\left(\frac{1}{2}|\nabla\psi_j|^2+(\kappa_j+V_j(\mathbf{x}))\,|\psi_j|^2-\psi_j^*\Omega L_z\psi_j+|\psi_j|^2\sum_{l=1}^{2}\beta_{j\,l}|\psi_l|^2\right)\\
&\quad\left.-\lambda\,\psi_j\psi_{k_j}^*+\lambda\,\psi_j^*\psi_{k_j}\right]d\mathbf{x}\\
&= i\lambda\int_{\mathbb{R}^d}\left(\psi_j^*\psi_{k_j}-\psi_j\psi_{k_j}^*\right)\,d\mathbf{x},\quad t\geq 0. \qquad (3.12)
\end{aligned}$$

Plugging (3.1) into (3.12), noticing (1.3), we obtain

$$N_1'(t) = i\lambda\int_{\mathbb{R}^d}\left(\psi_1^*\psi_2-\psi_1\psi_2^*\right)\,d\mathbf{x} = \lambda\,W_1(t), \qquad (3.13)$$

$$N_2'(t) = i\lambda\int_{\mathbb{R}^d}\left(\psi_2^*\psi_1-\psi_2\psi_1^*\right)\,d\mathbf{x} = -\lambda\,W_1(t), \qquad t\geq 0. \qquad (3.14)$$

Differentiating (3.1) with respect to t, noticing (2.1) and (2.5), we get

$$\begin{aligned}
W_1'(t) &= i\,\frac{d}{dt}\int_{\mathbb{R}^d}\left[\psi_1^*\psi_2-\psi_1\psi_2^*\right]\,d\mathbf{x}\\
&= i\int_{\mathbb{R}^d}\left[\psi_1^*\,\partial_t\psi_2+\psi_2\,\partial_t\psi_1^*-\psi_1\,\partial_t\psi_2^*-\psi_2^*\,\partial_t\psi_1\right]d\mathbf{x}\\
&= \int_{\mathbb{R}^d}\psi_1^*\left[\left(-\frac{1}{2}\nabla^2+\kappa_2+V_2(\mathbf{x})-\Omega L_z+\sum_{l=1}^{2}\beta_{2\,l}|\psi_l|^2\right)\psi_2-\lambda\psi_1\right]d\mathbf{x}\\
&\quad-\int_{\mathbb{R}^d}\psi_2\left[\left(-\frac{1}{2}\nabla^2+\kappa_1+V_1(\mathbf{x})-\Omega L_z^*+\sum_{l=1}^{2}\beta_{1\,l}|\psi_l|^2\right)\psi_1^*-\lambda\psi_2^*\right]d\mathbf{x}\\
&\quad+\int_{\mathbb{R}^d}\psi_1\left[\left(-\frac{1}{2}\nabla^2+\kappa_2+V_2(\mathbf{x})-\Omega L_z^*+\sum_{l=1}^{2}\beta_{2\,l}|\psi_l|^2\right)\psi_2^*-\lambda\psi_1^*\right]d\mathbf{x}\\
&\quad-\int_{\mathbb{R}^d}\psi_2^*\left[\left(-\frac{1}{2}\nabla^2+\kappa_1+V_1(\mathbf{x})-\Omega L_z+\sum_{l=1}^{2}\beta_{1\,l}|\psi_l|^2\right)\psi_1-\lambda\psi_2\right]d\mathbf{x}. \qquad (3.15)
\end{aligned}$$

Integrating by parts in (3.15), noticing (3.2), (2.5) and (3.10), we get

$$\begin{aligned} W_1'(t) &= \int_{\mathbb{R}^d} \Big[(\psi_1^*\psi_2 + \psi_1\psi_2^*) \Big(\kappa_2 - \kappa_1 + V_2(\mathbf{x}) - V_1(\mathbf{x}) + (\beta_{12} - \beta_{11})|\psi_1|^2 \\ &\quad + (\beta_{22} - \beta_{12})|\psi_2|^2 \Big) + 2\lambda \left(|\psi_2|^2 - |\psi_1|^2 \right) \Big] d\mathbf{x} \\ &= 2\lambda \left(N_2(t) - N_1(t) \right) + (\kappa_2 - \kappa_1) W_2(t) + F_1(t) \\ &= 2\lambda \left(1 - 2N_1(t) \right) + (\kappa_2 - \kappa_1) W_2(t) + F_1(t), \qquad t \geq 0. \end{aligned} \tag{3.16}$$

Similarly, differentiating (3.2) with respect to t, noticing (2.1), (3.1) and (3.11), integrating by parts, we get

$$\begin{aligned} W_2'(t) &= \frac{d}{dt} \int_{\mathbb{R}^d} \left[\psi_1^*\psi_2 + \psi_1\psi_2^* \right] \, d\mathbf{x} \\ &= \int_{\mathbb{R}^d} \left[\psi_2 \, \partial_t \psi_1^* + \psi_1^* \, \partial_t \psi_2 + \psi_1 \, \partial_t \psi_2^* + \psi_2^* \, \partial_t \psi_1 \right] d\mathbf{x} \\ &= i \int_{\mathbb{R}^d} \psi_2 \left[\left(-\frac{1}{2}\nabla^2 + \kappa_1 + V_1(\mathbf{x}) - \Omega L_z^* + \sum_{l=1}^{2} \beta_{1\,l} |\psi_l|^2 \right) \psi_1^* - \lambda \psi_2^* \right] d\mathbf{x} \\ &\quad - i \int_{\mathbb{R}^d} \psi_1^* \left[\left(-\frac{1}{2}\nabla^2 + \kappa_2 + V_2(\mathbf{x}) - \Omega L_z + \sum_{l=1}^{2} \beta_{2\,l} |\psi_l|^2 \right) \psi_2 - \lambda \psi_1 \right] d\mathbf{x} \\ &\quad + i \int_{\mathbb{R}^d} \psi_1 \left[\left(-\frac{1}{2}\nabla^2 + \kappa_2 + V_2(\mathbf{x}) - \Omega L_z^* + \sum_{l=1}^{2} \beta_{2\,l} |\psi_l|^2 \right) \psi_2^* - \lambda \psi_1^* \right] d\mathbf{x} \\ &\quad - i \int_{\mathbb{R}^d} \psi_2^* \left[\left(-\frac{1}{2}\nabla^2 + \kappa_1 + V_1(\mathbf{x}) - \Omega L_z + \sum_{l=1}^{2} \beta_{1\,l} |\psi_l|^2 \right) \psi_1 - \lambda \psi_2 \right] d\mathbf{x} \\ &= i \int_{\mathbb{R}^d} \Big[(\psi_1^*\psi_2 - \psi_1\psi_2^*) \Big(\kappa_1 - \kappa_2 + V_1(\mathbf{x}) - V_2(\mathbf{x}) + (\beta_{11} - \beta_{12})|\psi_1|^2 \\ &\quad + (\beta_{12} - \beta_{22})|\psi_2|^2 \Big) \Big] d\mathbf{x} \\ &= (\kappa_1 - \kappa_2) W_1(t) + F_2(t), \qquad t \geq 0. \end{aligned} \tag{3.17}$$

□

LEMMA 3.2. *Suppose that there is no external driving field in the CGPEs (2.1), i.e. $\lambda = 0$, then the density of each component is conserved, i.e.*

$$N_1(t) \equiv N_1(0) = \frac{N_1^0}{N}, \qquad N_2(t) \equiv N_2(0) = \frac{N_2^0}{N}, \qquad t \geq 0. \tag{3.18}$$

In addition, we have

(i) If the external trapping potentials are the same and the inter-/intra-component s-wave scattering lengths in (2.1) are the same, i.e.

$$V_1(\mathbf{x}) = V_2(\mathbf{x}), \quad \mathbf{x} \in \mathbb{R}^d, \quad \text{and} \quad \beta_{11} = \beta_{12} = \beta_{22} \ (\textit{i.e. } a_{11} = a_{12} = a_{22}), \tag{3.19}$$

then for any initial data $(\psi_1^0(\mathbf{x}), \psi_2^0(\mathbf{x}))$, we have

$$W_1(t) = W_1^{(0)} \cos\left((\kappa_1 - \kappa_2)t\right) - W_2^{(0)} \sin\left((\kappa_1 - \kappa_2)t\right), \tag{3.20}$$

$$W_2(t) = W_1^{(0)} \sin\left((\kappa_1 - \kappa_2)t\right) + W_2^{(0)} \cos\left((\kappa_1 - \kappa_2)t\right), \qquad t \geq 0. \tag{3.21}$$

This immediately implies that: (i) if $\kappa_1 = \kappa_2$, then $W_1(t) \equiv W_1^{(0)}$ and $W_2(t) \equiv W_2^{(0)}$ are two conserved quantities; and (ii) if $\kappa_1 \neq \kappa_2$, then $W_1(t)$ and $W_2(t)$ are periodic functions with period $T = 2\pi/|\kappa_1 - \kappa_2|$.

(ii) For all other cases, we have, for any $t \geq 0$,

$$W_1(t) = W_1^{(0)} \cos\left((\kappa_1 - \kappa_2)t\right) - W_2^{(0)} \sin\left((\kappa_1 - \kappa_2)t\right) + f_1(t), \tag{3.22}$$

$$W_2(t) = W_1^{(0)} \sin\left((\kappa_1 - \kappa_2)t\right) + W_2^{(0)} \cos\left((\kappa_1 - \kappa_2)t\right) + f_2(t), \qquad t \geq 0; \tag{3.23}$$

where $(f_1(t), f_2(t))$ is the solution of the following first-order ODE system:

$$f_1'(t) + (\kappa_1 - \kappa_2) f_2(t) = F_1(t), \tag{3.24}$$

$$f_2'(t) + (\kappa_2 - \kappa_1) f_1(t) = F_2(t), \qquad t \geq 0, \tag{3.25}$$

$$f_1(0) = f_2(0) = 0. \tag{3.26}$$

Proof. When $\lambda = 0$, the ODE system (3.3)-(3.5) collapses to

$$N_1'(t) = 0, \qquad N_2'(t) = 0, \tag{3.27}$$

$$W_1'(t) + (\kappa_1 - \kappa_2) W_2(t) = F_1(t), \qquad t > 0, \tag{3.28}$$

$$W_2'(t) + (\kappa_2 - \kappa_1) W_1(t) = F_2(t). \tag{3.29}$$

Thus (3.18) is a combination of (3.27), (3.6) and (3.7).

(i) When the conditions in (3.19) are satisfied, noticing (3.10), (3.11), we immediately obtain

$$F_1(t) \equiv 0, \qquad F_2(t) \equiv 0, \qquad t \geq 0. \tag{3.30}$$

Plugging (3.30) into (3.28) and (3.29), we have

$$W_1'(t) + (\kappa_1 - \kappa_2) W_2(t) = 0, \tag{3.31}$$

$$W_2'(t) + (\kappa_2 - \kappa_1) W_1(t) = 0, \qquad t \geq 0. \tag{3.32}$$

Thus (3.20)-(3.21) is the unique solution of the first-order ODE system (3.31)-(3.32) with the initial data (3.8) and (3.9).

(ii) From the results in (i) and using the superposition principle, we get that (3.22)-(3.23) is the unique solution of the first-order ODE system (3.28)-(3.29) with the initial data (3.8) and (3.9). □

LEMMA 3.3. *Suppose that there is an external driving field in the CGPEs (2.1), i.e. $\lambda \neq 0$,*

(i) If the external trapping potentials are the same and the inter-/intra-component s-wave scattering lengths in (2.1) are the same, i.e. the conditions in (3.19) are satisfied, we have

$$N_1(t) = \frac{C_0}{\omega^2} + \left(N_1^{(0)} - \frac{C_0}{\omega^2}\right) \cos(\omega t) + \frac{\lambda\, W_1^{(0)}}{\omega} \sin(\omega t), \tag{3.33}$$

$$N_2(t) = 1 - \frac{C_0}{\omega^2} - \left(N_1^{(0)} - \frac{C_0}{\omega^2}\right) \cos(\omega t) - \frac{\lambda\, W_1^{(0)}}{\omega} \sin(\omega t), \tag{3.34}$$

$$W_1(t) = W_1^{(0)} \cos(\omega t) + \left(\frac{C_0}{\lambda\omega} - \frac{\omega N_1^{(0)}}{\lambda}\right) \sin(\omega t), \tag{3.35}$$

$$W_2(t) = W_2^{(0)} + C_1\left[1 - \cos(\omega t)\right] + C_2 \sin(\omega t), \qquad t \geq 0; \tag{3.36}$$

where

$$\omega = \sqrt{4\lambda^2 + (\kappa_1 - \kappa_2)^2}, \quad C_0 = 2\lambda^2 + \lambda(\kappa_2 - \kappa_1)W_2^{(0)} + (\kappa_2 - \kappa_1)^2 N_1^{(0)}, \tag{3.37}$$

$$C_1 = \frac{\kappa_2 - \kappa_1}{\lambda}\left(N_1^{(0)} - \frac{C_0}{\omega^2}\right), \qquad C_2 = \frac{W_1^{(0)}(\kappa_1 - \kappa_2)}{\omega}. \tag{3.38}$$

These solutions immediately imply that $N_1(t)$, $N_2(t)$, $W_1(t)$ and $W_2(t)$ are periodic functions with period $T = 2\pi/\omega = 2\pi/\sqrt{4\lambda^2 + (\kappa_1 - \kappa_2)^2}$.

(ii) For all other cases, we have,

$$N_1(t) = \frac{C_0}{\omega^2} + \left(N_1^{(0)} - \frac{C_0}{\omega^2}\right)\cos(\omega t) + \frac{\lambda\, W_1^{(0)}}{\omega}\sin(\omega t) + f(t), \quad t \geq 0, \tag{3.39}$$

$$N_2(t) = 1 - \frac{C_0}{\omega^2} - \left(N_1^{(0)} - \frac{C_0}{\omega^2}\right)\cos(\omega t) - \frac{\lambda\, W_1^{(0)}}{\omega}\sin(\omega t) - f(t), \tag{3.40}$$

$$W_1(t) = W_1^{(0)}\cos(\omega t) + \left(\frac{C_0}{\lambda\omega} - \frac{\omega N_1^{(0)}}{\lambda}\right)\sin(\omega t) + \frac{1}{\lambda}f'(t), \tag{3.41}$$

$$W_2(t) = W_2^{(0)} + C_1\left[1 - \cos(\omega t)\right] + C_2\sin(\omega t) + \frac{\kappa_1 - \kappa_2}{\lambda}f(t) + \int_0^t F_2(\tau)\, d\tau; \tag{3.42}$$

where $f(t)$ is the solution of the following second-order ODE:

$$f''(t) + \omega^2 f(t) = \lambda\, F_1(t) + \lambda(\kappa_2 - \kappa_1)\int_0^t F_2(\tau)\, d\tau, \tag{3.43}$$

$$f(0) = f'(0) = 0. \tag{3.44}$$

Proof. When $\lambda \neq 0$, differentiating the first equation in (3.3) with respect to t, noticing (3.4), we obtain

$$\begin{aligned} N_1''(t) &= \lambda\, W_1'(t) \\ &= 2\lambda^2[1 - 2N_1(t)] + \lambda(\kappa_2 - \kappa_1)W_2(t) + \lambda\, F_1(t), \qquad t \geq 0. \end{aligned} \tag{3.45}$$

Plugging the first equation in (3.3) into (3.5), we have

$$W_2'(t) + \frac{\kappa_2 - \kappa_1}{\lambda}\, N_1'(t) = F_2(t), \qquad t \geq 0. \tag{3.46}$$

Solving the above first order ODE, noticing the initial conditions (3.6) and (3.9), we get

$$\begin{aligned} W_2(t) &= \frac{\kappa_1 - \kappa_2}{\lambda}\, N_1(t) + W_2(0) + \frac{\kappa_2 - \kappa_1}{\lambda}\, N_1(0) + \int_0^t F_2(\tau)\, d\tau \\ &= \frac{\kappa_1 - \kappa_2}{\lambda}\, N_1(t) + W_2^{(0)} + \frac{\kappa_2 - \kappa_1}{\lambda}\, N_1^{(0)} + \int_0^t F_2(\tau)\, d\tau, \qquad t \geq 0. \end{aligned} \tag{3.47}$$

Plugging (3.47) into (3.45), noticing (3.37), we have

$$N_1''(t) + \omega^2 N_1(t) = C_0 + \lambda\, F_1(t) + \lambda(\kappa_2 - \kappa_1)\int_0^t F_2(\tau)\, d\tau, \qquad t \geq 0. \tag{3.48}$$

(i) When the conditions in (3.19) are satisfied, we immediately obtain (3.30). Plugging (3.30) into (3.48), we obtain

$$N_1''(t) + \omega^2 N_1(t) = C_0, \qquad t \geq 0, \tag{3.49}$$

together with initial conditions

$$N_1(0) = N_1^{(0)}, \qquad N_1'(0) = \lambda\, W_1(0) = \lambda\, W_1^{(0)}. \tag{3.50}$$

Thus, (3.33) is the unique solution of the second-order ODE (3.49) with the initial data (3.50). Then the solution (3.34) is a combination of (3.33) and (2.5). Finally, plugging (3.33) into (3.3) and (3.47) with $F_2(\tau) \equiv 0$, we immediately get the solution (3.35) and (3.36), respectively.

(ii) From the results in (i) and using the superposition principle, we get that (3.39) is the unique solution of the second-order ODE (3.48) with the initial data (3.50). Then the solution (3.40) is a combination of (3.39) and (2.5). Finally, plugging (3.39) into (3.3) and (3.47), we immediately get the solution (3.41) and (3.42), respectively. □

3.2. Conservation of angular momentum expectation. As a measure of vortex flux, we define the total angular momentum expectation:

$$\langle L_z\rangle(t) = \langle L_z\rangle_1(t) + \langle L_z\rangle_2(t), \qquad t \geq 0, \tag{3.51}$$

where for $j = 1, 2$

$$\langle L_z\rangle_j(t) = \int_{\mathbb{R}^d} \psi_j^*(\mathbf{x},t) L_z \psi_j(\mathbf{x},t)\, d\mathbf{x} = i \int_{\mathbb{R}^d} \psi_j^*(\mathbf{x},t)(y\partial_x - x\partial_y)\psi_j(\mathbf{x},t)\, d\mathbf{x}. \tag{3.52}$$

In fact, $\langle \widetilde{L}_z\rangle_j(t) := \frac{\langle L_z\rangle_j(t)}{N_j(t)}$ is the angular momentum expectation of the jth ($j = 1, 2$) component. Typically when $\lambda = 0$, as the density of each component is conserved, then $\langle \widetilde{L}_z\rangle_j(t) = \frac{\langle L_z\rangle_j(t)}{N_j(0)}$. For the dynamics of the angular momentum expectations in rotating two-component BEC, we have the following lemmas.

LEMMA 3.4. *Suppose $(\psi_1(\mathbf{x},t), \psi_2(\mathbf{x},t))$ is the solution of the CGPEs (2.1)-(2.2); then we have,*

$$\begin{aligned} \frac{d\langle L_z\rangle_j(t)}{dt} &= \left(\gamma_{x,j}^2 - \gamma_{y,j}^2\right) \int_{\mathbb{R}^d} xy|\psi_j|^2\, d\mathbf{x} - \beta_{jk_j} \int_{\mathbb{R}^d} |\psi_j|^2 (x\partial_y - y\partial_x)|\psi_{k_j}|^2\, d\mathbf{x} \\ &\quad -2\lambda\, \mathrm{Re}\left[\int_{\mathbb{R}^d} \psi_{k_j}^*(x\partial_y - y\partial_x)\psi_j\, d\mathbf{x}\right], \quad t \geq 0, \quad j = 1, 2. \end{aligned} \tag{3.53}$$

Proof: The proof follows the line of the analogous result for the case of $\kappa_1 = \kappa_2 = 0$ in [**53**]. □

From the above lemma, we have

LEMMA 3.5. *Suppose the traps in (2.4) are radially symmetric in 2D, and resp. cylindrically symmetric in 3D, i.e. $\gamma_{x,1} = \gamma_{y,1}$ and $\gamma_{x,2} = \gamma_{y,2}$.*

(i) For any given initial data $\left(\psi_1^0(\mathbf{x}), \psi_2^0(\mathbf{x})\right)$ in (2.2), the total angular momentum expectation is conserved, i.e.

$$\langle L_z\rangle(t) \equiv \langle L_z\rangle(0) = \sum_{j=1}^{2} \int_{\mathbb{R}^d} \left(\psi_j^0(\mathbf{x})\right)^* L_z \psi_j^0(\mathbf{x})\, d\mathbf{x}, \qquad t \geq 0. \tag{3.54}$$

In addition, the energy for non-rotating part is also conserved, i.e.

$$E_n(\psi_1,\psi_2) := \int_{\mathbb{R}^d}\left[\sum_{j=1}^{2}\left(\frac{1}{2}|\nabla\psi_j|^2+(\kappa_j+V_j(\mathbf{x}))\,|\psi_j|^2+\sum_{l=1}^{2}\frac{\beta_{jl}}{2}|\psi_j|^2|\psi_l|^2\right)\right.$$

$$\left.-2\lambda\,\mathrm{Re}(\psi_1^*\psi_2)\right]d\mathbf{x}\equiv E_n\left(\psi_1^0,\psi_2^0\right),\qquad t\geq 0. \tag{3.55}$$

(ii) Suppose the initial data $(\psi_1^0(\mathbf{x}),\psi_2^0(\mathbf{x}))$ in (2.2) is chosen as

$$\psi_j^0(\mathbf{x})=f_j(r)e^{im_j\theta}\quad \textit{with}\quad m_j\in\mathbb{Z}\quad \textit{and}\quad f_j(0)=0\quad \textit{when}\quad m_j\neq 0, \tag{3.56}$$

in 2D, and resp. in 3D,

$$\psi_j^0(\mathbf{x})=f_j(r,z)e^{im_j\theta}\quad \textit{with}\quad m_j\in\mathbb{Z}\quad \textit{and}\quad f_j(0,z)=0\quad \textit{when}\quad m_j\neq 0. \tag{3.57}$$

If $\lambda=0$, then $\langle\widetilde{L}_z\rangle_1(t)$ and $\langle\widetilde{L}_z\rangle_2(t)$ are conserved, i.e.

$$\langle\widetilde{L}_z\rangle_j(t)\equiv\langle\widetilde{L}_z\rangle_j(0)=\frac{1}{N_j(0)}\int_{\mathbb{R}^d}\left(\psi_j^0(\mathbf{x})\right)^* L_z\psi_j^0(\mathbf{x})\,d\mathbf{x},\quad t\geq 0,\ \ j=1,2. \tag{3.58}$$

On the other hand, if $m_1=m_2:=m$ in (3.56) for 2D, and resp. in (3.57) for 3D, then for any given λ, $\langle\widetilde{L}_z\rangle_1(t)$ and $\langle\widetilde{L}_z\rangle_2(t)$ are conserved, i.e.

$$\langle\widetilde{L}_z\rangle_j(t)\equiv\langle\widetilde{L}_z\rangle_j(0)=m,\qquad t\geq 0,\quad j=1,2. \tag{3.59}$$

Proof: Again, the proof follows the line of the analogous result for the case of $\kappa_1=\kappa_2=0$ in [**53**]. □

3.3. Dynamics of condensate widths. Another important quantity characterizing the dynamics of a rotating two-component BEC is the condensate width defined as

$$\sigma_\alpha(t)=\sqrt{\delta_\alpha(t)}=\sqrt{\delta_{\alpha,1}(t)+\delta_{\alpha,2}(t)},\qquad \alpha=x,y\text{ or }z, \tag{3.60}$$

where

$$\delta_{\alpha,j}(t)=\langle\alpha^2\rangle_j(t)=\int_{\mathbb{R}^d}\alpha^2|\psi_j(\mathbf{x},t)|^2\,d\mathbf{x},\qquad t\geq 0,\qquad j=1,2. \tag{3.61}$$

For the dynamics of condensate widths, we have the following lemmas.

LEMMA 3.6. *Suppose $(\psi_1(\mathbf{x},t),\psi_2(\mathbf{x},t))$ is the solution of problem (2.1)-(2.2); then we have*

$$\frac{d^2\delta_\alpha(t)}{dt^2} = \int_{\mathbb{R}^d}\sum_{j=1}^{2}\Big[(\partial_y\alpha-\partial_x\alpha)\left(4i\Omega\psi_j^*(x\partial_y+y\partial_x)\psi_j+2\Omega^2(x^2-y^2)|\psi_j|^2\right)$$

$$+2|\partial_\alpha\psi_j|^2-2\alpha|\psi_j|^2\partial_\alpha(V_j(\mathbf{x}))+|\psi_j|^2\sum_{l=1}^{2}\beta_{jl}|\psi_l|^2\Big]d\mathbf{x},\ \ t\geq 0, \tag{3.62}$$

with initial conditions

$$\delta_\alpha(0)=\delta_\alpha^{(0)}=\int_{\mathbb{R}^d}\alpha^2\left(|\psi_1^0(\mathbf{x})|^2+|\psi_2^0(\mathbf{x})|^2\right)d\mathbf{x},\qquad \alpha=x,y,z, \tag{3.63}$$

$$\delta'_\alpha(0) = \delta_\alpha^{(1)} = 2\sum_{j=1}^{2}\int_{\mathbb{R}^d} \alpha\left[-\Omega|\psi_j^0|^2\left(x\partial_y - y\partial_x\right)\alpha + \mathrm{Im}\left((\psi_j^0)^*\partial_\alpha\psi_j^0\right)\right]\, d\mathbf{x}. \tag{3.64}$$

Proof: The proof follows the line of the analogous result for the case of $\kappa_1 = \kappa_2 = 0$ in [**53**]. □

From the above lemma, we have

LEMMA 3.7. *In 2D with radially symmetric traps, i.e., $d = 2$, $\kappa_1 = \kappa_2$ and $\gamma_{x,1} = \gamma_{y,1} = \gamma_{x,2} = \gamma_{y,2} := \gamma_r$ in (2.1), we have*

(i) If there is no external driving field, i.e. $\lambda = 0$ in (2.1), for any given initial data $(\psi_1^0(\mathbf{x}), \psi_2^0(\mathbf{x}))$ in (2.2), we have, for $t \geq 0$,

$$\begin{aligned}\delta_r(t) &= \frac{E(\psi_1^0,\psi_2^0) + \Omega\langle L_z\rangle(0) - \kappa_1}{\gamma_r^2}\left[1-\cos(2\gamma_r t)\right] \\ &\quad + \delta_r^{(0)}\cos(2\gamma_r t) + \frac{\delta_r^{(1)}}{2\gamma_r}\sin(2\gamma_r t),\end{aligned} \tag{3.65}$$

where $\delta_r(t) = \delta_x(t) + \delta_y(t)$, $\delta_r^{(0)} := \delta_x(0) + \delta_y(0)$ and $\delta_r^{(1)} := \delta'_x(0) + \delta'_y(0)$. Furthermore, when the initial data $(\psi_1^0(\mathbf{x}), \psi_2^0(\mathbf{x}))$ in (2.2) satisfies (3.56) with $m_1 = m_2$, we have, for $t \geq 0$,

$$\begin{aligned}\delta_x(t) &= \delta_y(t) = \frac{1}{2}\delta_r(t) \\ &= \frac{E\left(\psi_1^0,\psi_2^0\right) + \Omega\langle L_z\rangle(0) - \kappa_1}{2\gamma_r^2}[1-\cos(2\gamma_r t)] \\ &\quad + \delta_x^{(0)}\cos(2\gamma_r t) + \frac{\delta_x^{(1)}}{2\gamma_r}\sin(2\gamma_r t).\end{aligned} \tag{3.66}$$

Thus in this case, the condensate widths $\sigma_r(t)$, $\sigma_x(t)$ and $\sigma_y(t)$ are periodic functions with frequency doubling the trapping frequency.

(ii) If there is an external driving field, i.e. $\lambda \neq 0$ in (2.1), we have

$$\begin{aligned}\delta_r(t) &= \frac{E(\psi_1^0,\psi_2^0) + \Omega\langle L_z\rangle(0) - \kappa_1}{\gamma_r^2} + \frac{\delta_r^{(1)}}{2\gamma_r}\sin(2\gamma_r t) + g_r(t) \\ &\quad + \left(\delta_r^{(0)} - \frac{E(\psi_1^0,\psi_2^0) + \Omega\langle L_z\rangle(0) - \kappa_1}{\gamma_r^2}\right)\cos(2\gamma_r t), \qquad t \geq 0,\end{aligned} \tag{3.67}$$

where $g_r(t)$ is the solution of the following second-order ODE:

$$\frac{d^2 g_r(t)}{dt^2} + 4\gamma_r^2\, g_r(t) = G_r(t), \qquad g_r(0) = g'_r(0) = 0, \tag{3.68}$$

with

$$G_r(t) = 4\int_{\mathbb{R}^d}\left[\lambda\left(\psi_1^*\psi_2 + \psi_1\psi_2^*\right) + (\kappa_1 - \kappa_2)|\psi_2|^2\right] d\mathbf{x}.$$

Proof: Again, the proof follows the line of the analogous result for the case of $\kappa_1 = \kappa_2 = 0$ in [**53**]. □

3.4. Dynamics of a stationary state with its centers shifted. When $\lambda = 0$ in (2.1), let $(\phi_1^e(\mathbf{x}), \phi_2^e(\mathbf{x}))$ be a stationary state of the CGPEs (2.1) with chemical potential (μ_1^e, μ_2^e), i.e., $(\mu_1^e, \mu_2^e; \phi_1^e, \phi_2^e)$ satisfying

$$\mu_j^e\ \phi_j^e(\mathbf{x}) = -\frac{1}{2}\nabla^2\phi_j^e + (\kappa_j + V_j(\mathbf{x}))\,\phi_j^e - \Omega\ L_z\phi_j^e + \sum_{l=1}^{2}\beta_{jl}|\phi_l^e|^2\phi_j^e,\ \ \mathbf{x}\in\mathbb{R}^d, \tag{3.69}$$

$$\|\phi_j^e\|^2 := \int_{\mathbb{R}^d} |\phi_j^e(\mathbf{x})|^2\ d\mathbf{x} = \frac{N_j^0}{N}, \quad j = 1, 2. \tag{3.70}$$

If the initial data $(\psi_1^0(\mathbf{x}), \psi_2^0(\mathbf{x}))$ in (2.2) is chosen as a stationary state with a shift in its center, one can construct an exact solution of the CGPEs (2.1) with harmonic oscillator potentials (2.4). This kind of analytical construction can be used, in particular, in the benchmark and validation of numerical algorithms for the CGPEs (2.1). For single-component non-rotating and rotating BEC, this kind of analytical construction can be found in the literature [**23, 5**]. For rotating two-component BEC, we have the following lemma.

LEMMA 3.8. *If the initial data $(\psi_1^0(\mathbf{x}), \psi_2^0(\mathbf{x}))$ in (2.2) is chosen as*

$$\psi_1^0(\mathbf{x}) = \phi_1^e(\mathbf{x} - \mathbf{x}_1^0), \quad \psi_2^0(\mathbf{x}) = \phi_2^e(\mathbf{x} - \mathbf{x}_2^0), \qquad \mathbf{x}\in\mathbb{R}^d, \tag{3.71}$$

where $\mathbf{x}_1^0$ and $\mathbf{x}_2^0$ are two given points in $\mathbb{R}^d$, when $\lambda = 0$, $\mathbf{x}_1^0 = \mathbf{x}_2^0 := \mathbf{x}^0$ and $V_1(\mathbf{x}) \equiv V_2(\mathbf{x})$, then the exact solution of the CGPEs (2.1)-(2.2) satisfies

$$\psi_j(\mathbf{x}, t) = \phi_j^e(\mathbf{x} - \mathbf{x}(t))e^{-i\mu_j^e t}e^{iw_j(\mathbf{x},t)}, \quad \mathbf{x}\in\mathbb{R}^d, \quad t \ge 0, \quad j = 1, 2, \tag{3.72}$$

where for any $t \ge 0$, $w_j(\mathbf{x}, t)$ is a linear function for $\mathbf{x}$, i.e. for $j = 1, 2$

$$w_j(\mathbf{x}, t) = \mathbf{c}_j(t)\cdot\mathbf{x} + g_j(t), \quad \mathbf{c}_j(t) = (c_{j,1}(t), \cdots, c_{j,d}(t))^T, \quad \mathbf{x}\in\mathbb{R}^d, \quad t \ge 0, \tag{3.73}$$

and $\mathbf{x}(t)$ satisfies the following second-order ODE system

$$x''(t) - 2\Omega y'(t) + \left(\gamma_{x,1}^2 - \Omega^2\right)x(t) = 0, \tag{3.74}$$

$$y''(t) + 2\Omega x'(t) + \left(\gamma_{y,1}^2 - \Omega^2\right)y(t) = 0, \qquad t \ge 0, \tag{3.75}$$

$$x(0) = x^0, \quad y(0) = y^0, \quad x'(0) = \Omega y^0, \quad y'(0) = -\Omega x^0. \tag{3.76}$$

Moreover, if in 3D, another ODE needs to be added:

$$z''(t) + \gamma_{z,1}^2\, z(t) = 0, \quad z(0) = z^0, \quad z'(0) = 0. \tag{3.77}$$

Proof: The proof follows the line of the analogous result for the case of $\kappa_1 = \kappa_2 = 0$ in [**53**]. □

The ODE system (3.74)-(3.77) governing the motion of the center of mass $\mathbf{x}(t)$ [**52**] for rotating two-component BEC is the same as that for single-component BEC [**5**]. This ODE system was solved analytically in [**52**] and different motion patterns of the center were classified in details based on the parameters Ω, $\gamma_{x,1}$, $\gamma_{y,1}$ and $\gamma_{z,1}$.

4. Numerical methods

In this section, we review efficient and accurate numerical methods for solving the CGPEs (2.1)-(2.2) for the dynamics of two-component BEC. The key ideas are: (i) to apply a time-splitting technique for decoupling the nonlinearity; and (ii) to adopt the Cartesian coordinates and the polar coordinates in 2D (and resp.

cylindrical coordinates in 3D) for nonrotating and rotating two-component BEC, respectively. Due to the trapping potentials $V_1(\mathbf{x})$ and $V_2(\mathbf{x})$ given by (2.4), the solution (ψ_1, ψ_2) of (2.1)-(2.2) decays to zero exponentially fast when $|\mathbf{x}| \to \infty$. Thus in practical computation, we truncate the problem (2.1)-(2.2) into a bounded computational domain $\Omega_{\mathbf{x}}$ with homogeneous Dirichlet boundary conditions:

$$i\frac{\partial \psi_j}{\partial t} = \left[-\frac{1}{2}\nabla^2 + \kappa_j + V_j(\mathbf{x}) - \Omega L_z + \sum_{l=1}^{2}\beta_{jl}|\psi_l|^2\right]\psi_j - \lambda\psi_{k_j},\ t \geq 0, \tag{4.1}$$

$$\psi_j(\mathbf{x}, t) = 0,\ \mathbf{x} \in \Gamma = \partial\Omega_{\mathbf{x}},\ t \geq 0, \tag{4.2}$$

$$\psi_j(\mathbf{x}, 0) = \psi_j^0(\mathbf{x}), \quad \mathbf{x} \in \overline{\Omega}_{\mathbf{x}}, \quad \text{with} \quad \int_{\Omega_{\mathbf{x}}} \left(|\psi_1^0(\mathbf{x})|^2 + |\psi_2^0(\mathbf{x})|^2\right)\, d\mathbf{x} = 1. \tag{4.3}$$

In practical computation, we use sufficiently large domain so as to make sure the homogeneous Dirichlet boundary condition (4.2) doesn't introduce aliasing error. Usually, the radius of the bounded computational domain depends on the problem. In general, it should be larger than the "Thomas-Fermi radius". Of course, the use of more sophisticated radiation boundary conditions is an interesting topic that remains to be examined in the future.

4.1. For nonrotating two-component BEC. In this case, i.e. $\Omega = 0$ in (4.1), we adopt the Cartesian coordinates and use the sine pseudospectral method for solving the linear Schrödinger equations.

Time-splitting We choose a time step $\Delta t > 0$. For $n = 0, 1, \ldots,$ from time $t = t_n = n\Delta t$ to $t = t_{n+1} = t_n + \Delta t$, the CGPEs (4.1) with $\Omega = 0$ is solved in two splitting steps [**4, 7**]. One first solves

$$i\frac{\partial \psi_j}{\partial t} = -\frac{1}{2}\nabla^2\psi_j - \lambda\psi_{k_j}, \qquad j = 1, 2 \tag{4.4}$$

for the time step of length Δt, followed by solving

$$i\frac{\partial \psi_j}{\partial t} = \left(\kappa_j + V_j(\mathbf{x})\right)\psi_j + \sum_{l=1}^{2}\beta_{jl}|\psi_l|^2\psi_j, \qquad j = 1, 2 \tag{4.5}$$

for the same time step. For time $t \in [t_n, t_{n+1}]$, the ODE system (4.5) leaves $|\psi_1(\mathbf{x}, t)|$ and $|\psi_2(\mathbf{x}, t)|$ invariant in t [**4, 7**], and thus it can be integrated *exactly* to obtain [**4, 5**], for $j = 1, 2$ and $t \in [t_n, t_{n+1}]$

$$\psi_j(\mathbf{x}, t) = \psi_j(\mathbf{x}, t_n)\exp\left[-i\left(\kappa_j + V_j(\mathbf{x}) + \sum_{l=1}^{2}\beta_{jl}\left|\psi_l(\mathbf{x}, t_n)\right|^2\right)(t - t_n)\right]. \tag{4.6}$$

The equations (4.1) with $\Omega = 0$ are now decoupled and thus we need only show how to discretize (4.4). Various algorithms were introduced in the literature for discretizating the GPE (4.4) [**4, 9**]. For the convenience of the reader, here we review a method which discretizes the equation (4.10) by using sine pseudospectral method. In order to do so, we choose the bounded computational domain $\Omega_{\mathbf{x}} = (a, b)$ in 1D, $\Omega_{\mathbf{x}} = (a, b) \times (c, d)$ in 2D, and resp. $\Omega_{\mathbf{x}} = (a, b) \times (c, d) \times (e, f)$ in 3D with $|a|$, b, $|c|$, d, $|e|$ and f sufficiently large. For simplicity, we only present the method in 1D. Extensions to 2D and 3D are straightforward by tensor products.

Numerical algorithm In 1D, the equations (4.4) will be discretized in space by the sine-spectral method and integrated in time *exactly*. We choose the spatial mesh size $h = \Delta x = (b-a)/M$ with M an even positive integer and define the grid points by

$$x_m = a + m\,h, \qquad m = 0, 1, 2, \ldots, M.$$

Let $\left(\psi_{1,m}^n, \psi_{2,m}^n\right)$ be the approximation of $(\psi_1(x_m, t_n), \psi_2(x_m, t_n))$ for $m = 0, 1, 2, \ldots, M$ and denote (ψ_1^n, ψ_2^n) be the solution vector at time $t = t_n$ with component $\left(\psi_{1,m}^n, \psi_{2,m}^n\right)$. From time $t = t_n$ to $t = t_{n+1}$, we combine the splitting steps via the standard second-order splitting:

$$\begin{aligned}
\psi_{1,m}^{(1)} &= \psi_{1,m}^n\, e^{-i\Delta t\left(\kappa_1 + V_1(x_m) + \beta_{11}|\psi_{1,m}^n|^2 + \beta_{12}|\psi_{2,m}^n|^2\right)/2},\\
\psi_{2,m}^{(1)} &= \psi_{2,m}^n\, e^{-i\Delta t\left(\kappa_2 + V_2(x_m) + \beta_{12}|\psi_{1,m}^n|^2 + \beta_{22}|\psi_{2,m}^n|^2\right)/2},\\
\psi_{1,m}^{(2)} &= \frac{2}{M}\sum_{l=1}^{M-1} e^{-i\Delta t\mu_l^2/2}\left[\cos(\lambda\Delta t)\widehat{(\psi_1^{(1)})}_l + i\sin(\lambda\Delta t)\widehat{(\psi_2^{(1)})}_l\right]\,\sin\left(\frac{m\,l\,\pi}{M}\right),\\
\psi_{2,m}^{(2)} &= \frac{2}{M}\sum_{l=1}^{M-1} e^{-i\Delta t\mu_l^2/2}\left[i\sin(\lambda\Delta t)\widehat{(\psi_1^{(1)})}_l + \cos(\lambda\Delta t)\widehat{(\psi_2^{(1)})}_l\right]\,\sin\left(\frac{m\,l\,\pi}{M}\right),\\
\psi_{1,m}^{n+1} &= \psi_{1,m}^{(2)}\, e^{-i\Delta t\left(\kappa_1 + V_1(x_m) + \beta_{11}|\psi_{1,m}^{(2)}|^2 + \beta_{12}|\psi_{2,m}^{(2)}|^2\right)/2},\\
\psi_{2,m}^{n+1} &= \psi_{2,m}^{(2)}\, e^{-i\Delta t\left(\kappa_2 + V_2(x_m) + \beta_{12}|\psi_{1,m}^{(2)}|^2 + \beta_{22}|\psi_{2,m}^{(2)}|^2\right)/2}, \quad m = 1, 2, \ldots, M-1;
\end{aligned}$$

where $\hat{\phi}_l$ $(l = 1, 2, \ldots, M-1)$, the sine-transform coefficients of the vector $\Phi = (\phi_0, \phi_1, \phi_2, \ldots, \phi_M)^T$ with $\phi_0 = \phi_M = 0$, are defined as

$$\mu_l = \frac{l\pi}{b-a}, \quad \hat{\phi}_l = \sum_{m=1}^{M-1}\phi_m\,\sin\left(\frac{m\,l\,\pi}{M}\right),\ l = 1, 2, \ldots, M-1. \tag{4.7}$$

The overall time discretization error comes solely from the splitting, which is second order in time step Δt, and the spatial discretization is of spatial order of accuracy. The discretization is time reversible and time transverse invariant. Furthermore, for the stability of the above discretization, we have the following lemma, which shows that the total mass of the two-component BEC is conserved for any $\lambda \in \mathbb{R}$, and the mass of each component is conserved when there is no external driving field, i.e. $\lambda = 0$.

LEMMA 4.1. *The above time-splitting spectral method for nonrotating two-component BEC is unconditionally stable and conserves the total mass of two-component BEC. In fact, for any mesh size $h > 0$ and time step $\Delta t > 0$, we have*

$$\begin{aligned}
\|\psi_1^n\|^2 + \|\psi_2^n\|^2 &:= h\sum_{m=1}^{M-1}\left[|\psi_{1,m}^n|^2 + |\psi_{2,m}^n|^2\right]\\
&\equiv h\sum_{m=1}^{M-1}\left[|\psi_1^0(x_m)|^2 + |\psi_2^0(x_m)|^2\right], \quad n \ge 0.
\end{aligned} \tag{4.8}$$

Furthermore, when $\lambda = 0$ in (4.1), without the external driving field, we have

$$\|\psi_j^n\|^2 := h\sum_{m=1}^{M-1}|\psi_{j,m}^n|^2 \equiv h\sum_{m=1}^{M-1}|\psi_j^0(x_m)|^2, \quad n \geq 0, \qquad j = 1, 2. \tag{4.9}$$

Proof: The proof follows the line of the analogous result for the case of $\kappa_1 = \kappa_2 = 0$ in [**4**]. □

REMARK 4.2. When the external potentials $V_1(\mathbf{x})$ and $V_2(\mathbf{x})$ are chosen as the harmonic potentials, one can also solve the coupled Gross-Pitaevskii equations (4.1) with $\Omega = 0$ by using the time-splitting Laguerre-Hermite pseudo-spectral method proposed in [**9**].

4.2. For rotating two-component BEC. In this case, i.e. $\Omega \neq 0$ in (4.1), we adopt the polar coordinates in 2D, and resp. cylindrical coordinates in 3D, such that the angular momentum rotation term becomes a term with constant coefficients.

Time-splitting For $n = 0, 1, \ldots,$ from time $t = t_n = n\Delta t$ to $t = t_{n+1} = t_n + \Delta t$, the CGPEs (4.1) are solved in three splitting steps [**4, 7**]. One first solves

$$i\frac{\partial \psi_j}{\partial t} = -\frac{1}{2}\nabla^2\psi_j - \Omega L_z\psi_j, \qquad j = 1, 2 \tag{4.10}$$

for the time step of length Δt, followed by solving

$$i\frac{\partial \psi_j}{\partial t} = (\kappa_j + V_j(\mathbf{x}))\,\psi_j + \sum_{l=1}^{2}\beta_{jl}|\psi_l|^2\psi_j, \qquad j = 1, 2 \tag{4.11}$$

for the same time step, and then by solving

$$i\frac{\partial \psi_j}{\partial t} = -\lambda\psi_{k_j}, \qquad j = 1, 2 \tag{4.12}$$

again for the same time step. The solutions for (4.11) are given in (4.6). For the ODE system (4.12), we can rewrite it as

$$i\frac{\partial \Psi}{\partial t} = -\lambda A\Psi, \quad \text{with } A = \begin{pmatrix} 0 & 1 \\ 1 & 0 \end{pmatrix} \quad \textit{and} \quad \Psi = \begin{pmatrix} \psi_1 \\ \psi_2 \end{pmatrix}. \tag{4.13}$$

Since A is a real and symmetric matrix, it can be diagonalized and integrated *exactly*, and then we obtain [**4**], for $t \in [t_n, t_{n+1}]$

$$\Psi(\mathbf{x}, t) = e^{i\lambda A\,(t-t_n)}\Psi(\mathbf{x}, t_n) = \begin{pmatrix} \cos(\lambda(t-t_n)) & i\sin(\lambda(t-t_n)) \\ i\sin(\lambda(t-t_n)) & \cos(\lambda(t-t_n)) \end{pmatrix}\Psi(\mathbf{x}, t_n). \tag{4.14}$$

The equations (4.1) are now decoupled and thus we need only show how to discretize the following single GPE in a rotational frame:

$$i\frac{\partial \psi}{\partial t} = -\frac{1}{2}\nabla^2\psi - \Omega L_z\psi, \qquad \mathbf{x} \in \Omega_{\mathbf{x}}, \quad t_n \leq t \leq t_{n+1}. \tag{4.15}$$

Various algorithms were introduced in the literature for discretizating the GPE (4.15) [**5, 52, 10**]. For the convenience of the reader, here we review a method which discretizes the equation (4.15) in the θ-direction by the Fourier pseudospectral method, in the r-direction by the fourth-order finite difference method, in the z-direction by the sine pseudospectral method and in time by the Crank-Nicolson (C-N) scheme [**5, 53**]. In order to do so, we choose the bounded computational

domain $\Omega_{\mathbf{x}} = \{(x, y),\ r = \sqrt{x^2+y^2} < R\}$ in 2D, and resp. $\Omega_{\mathbf{x}} = \{(x, y, z),\ r = \sqrt{x^2+y^2} < R,\ a < z < b\}$ in 3D with R, $|a|$, and b sufficiently larger than the Thomas-Fermi radii.

Discretization in 2D When $d = 2$, we use the polar coordinate (r, θ) and assume that

$$\psi(r, \theta, t) = \sum_{l=-L/2}^{L/2-1} \widehat{\psi}_l(r, t) e^{il\theta}, \tag{4.16}$$

where L is an even positive integer and $\widehat{\psi}_l(r, t)$ is the Fourier coefficient for the l-th mode. Plugging (4.16) into (4.15) and noticing the orthogonality of the Fourier functions, we obtain, for $-\frac{L}{2} \le l \le \frac{L}{2} - 1$ and $0 < r < R$:

$$i\frac{\partial \widehat{\psi}_l(r,t)}{\partial t} = -\frac{1}{2r}\frac{\partial}{\partial r}\left(r\frac{\partial \widehat{\psi}_l(r,t)}{\partial r}\right) + \left(\frac{l^2}{2r^2} - l\Omega\right)\widehat{\psi}_l(r,t), \tag{4.17}$$

$$\widehat{\psi}_l(R,t) = 0, \quad (\text{for all } l), \qquad \widehat{\psi}_l(0,t) = 0, \quad (\text{for } l \neq 0). \tag{4.18}$$

In order to discretize (4.17)-(4.18) in space by the finite difference method, we choose an integer $M > 0$, a mesh size $\Delta r = 2R/(2M+1)$ and grid points $r_m = (m - 1/2)\Delta r$ for $1 \le m \le M+1$. Let $\widehat{\psi}_{l,m}(t)$ be the approximation of $\widehat{\psi}_l(r_m, t)$. Then a fourth-order finite difference discretization for (4.17)-(4.18) with $t \in [t_n, t_{n+1}]$ reads [**5, 34**]

$$\begin{aligned} i\frac{d\widehat{\psi}_{l,m}(t)}{dt} &= \left(\frac{l^2}{2r_m^2} - l\Omega\right)\widehat{\psi}_{l,m}(t) \\ &\quad - \frac{-\widehat{\psi}_{l,m+2}(t) + 16\widehat{\psi}_{l,m+1}(t) - 30\widehat{\psi}_{l,m}(t) + 16\widehat{\psi}_{l,m-1}(t) - \widehat{\psi}_{l,m-2}(t)}{24(\Delta r)^2} \\ &\quad - \frac{-\widehat{\psi}_{l,m+2}(t) + 8\widehat{\psi}_{l,m+1}(t) - 8\widehat{\psi}_{l,m-1}(t) + \widehat{\psi}_{l,m-2}(t)}{24 r_m \Delta r}, \quad 1 \le m \le M, \end{aligned} \tag{4.19}$$

$$\begin{aligned} i\frac{d\widehat{\psi}_{l,M+1}(t)}{dt} &= \left(\frac{l^2}{2r_{M+1}^2} - l\Omega\right)\widehat{\psi}_{l,M+1}(t) \\ &\quad - \frac{11\widehat{\psi}_{l,M+2}(t) - 20\widehat{\psi}_{l,M+1}(t) + 6\widehat{\psi}_{l,M}(t) + 4\widehat{\psi}_{l,M-1}(t) - \widehat{\psi}_{l,M-2}(t)}{24\,(\Delta r)^2} \\ &\quad - \frac{3\widehat{\psi}_{l,M+2}(t) + 10\widehat{\psi}_{l,M+1}(t) - 18\widehat{\psi}_{l,M}(t) + 6\widehat{\psi}_{l,M-1}(t) - \widehat{\psi}_{l,M-2}(t)}{24\, r_{M+1}\, \Delta r}, \end{aligned} \tag{4.20}$$

$$\widehat{\psi}_{l,-1}(t) = (-1)^l \widehat{\psi}_{l,2}(t), \quad \widehat{\psi}_{l,0}(t) = (-1)^l \widehat{\psi}_{l,1}(t), \quad \widehat{\psi}_{l,M+1}(t) = 0. \tag{4.21}$$

Finally, the ODE system (4.19)-(4.21) is discretized by the standard C-N scheme in time. Although an implicit time discretization is applied for (4.19)-(4.21), the one-dimensional nature of the problem makes the coefficient matrix for the linear system pentadiagonal, which can be solved very efficiently, i.e. via $O(M)$ arithmetic operations.

In practice, we always use the second-order Strang splitting [**49**]; i.e. from time $t = t_n$ to $t = t_{n+1}$ (i) evolve (4.11) for half time step $\Delta t/2$ with the initial data given at $t = t_n$; (ii) evolve (4.12) for half time step $\Delta t/2$ with the new data; (iii) evolve (4.10) for time step Δt with the new data obtained in (ii); (iv) evolve (4.12)

for half time step $\Delta t/2$ with the new data obtained in (iii), and (v) evolve (4.11) for half time step $\Delta t/2$ with the newer data.

For the discretization considered here, the total memory requirement is $O(ML)$ and the total computational cost per time step is $O(ML\ln L)$. The method is time reversible and time transverse invariant when the original CGPEs (2.1) does. Furthermore, following the similar proofs in [**4, 7, 5**], the total density can be shown to be conserved in the discretized level.

REMARK 4.3. When $\lambda = 0$ in (4.1), in the above second-order Strang splitting for the problem, the step (ii) and (iv) can be removed, and then the method will consist of three steps. In this case, the density of each component is also conserved in the discretized level. In addition, a second-order finite difference discretization for (4.17)-(4.18) was proposed in [**5**].

Discretization in 3D When $d = 3$, we use the cylindrical coordinate (r, θ, z) and assume that

$$\psi(r,\theta,z,t) = \sum_{l=-L/2}^{L/2-1} \sum_{k=1}^{K-1} \widehat{\psi}_{l,k}(r,t)\ e^{il\theta}\ \sin(\mu_k(z-a)), \tag{4.22}$$

where L and K are two even positive integers, $\mu_k = \frac{\pi k}{b-a}$ $(k = 1, \cdots, K-1)$ and $\widehat{\psi}_{l,k}(r,t)$ is the Fourier-sine coefficient for the (l,k)th mode. Plugging (4.22) into (4.15) with $d = 3$, noticing the orthogonality of the Fourier-sine modes, we obtain, for $-\frac{L}{2} \le l \le \frac{L}{2} - 1$, $1 \le k \le K-1$ and $0 < r < R$, that

$$i\frac{\partial \widehat{\psi}_{l,k}(r,t)}{\partial t} = -\frac{1}{2r}\frac{\partial}{\partial r}\left(r\frac{\partial \widehat{\psi}_{l,k}(r,t)}{\partial r}\right) + \left(\frac{l^2}{2r^2} + \frac{\mu_k^2}{2} - l\Omega\right)\widehat{\psi}_{l,k}(r,t), \tag{4.23}$$

with essential boundary conditions

$$\widehat{\psi}_{l,k}(R,t) = 0 \text{ (for all } l), \qquad \widehat{\psi}_{l,k}(0,t) = 0 \text{ (for } l \neq 0). \tag{4.24}$$

The discretization of (4.23)-(4.24) is similar as that for (4.17)-(4.18) and thus omitted here.

For the algorithm in 3D, the total memory requirement is $O(MLK)$ and the total computational cost per time step is $O(MLK\ln(LK))$.

REMARK 4.4. Another way to discretize the coupled GPEs (4.1) in the rotational frame is to use the efficient and accurate numerical method proposed in [**10**] for rotating single-component BEC. The key ideas are to apply a time-splitting for decoupling the nonlinearity and to properly use the alternating direction implicit (ADI) technique for the coupling in the angular momentum rotation terms in the GPEs, at each time step, the GPEs in rotational frame is decoupled into a nonlinear ordinary differential equations (ODEs) and two systems of partial differential equations with constant coefficients. For more details, we refer to [**10**].

5. Numerical results

For the completeness and convenience of the readers, here we also present some numerical results for the dynamics of rotating two-component BEC [**53**]. For more numerical results, one can refer to [**4, 9, 53**].

Example 1. Dynamics of the density of each component [**53**], we take $d = 2$, $\kappa_1 = \kappa_2 = 0$, $\lambda = 1$, $\Omega = 0.6$, $\gamma_{x,j} = \gamma_{y,j} = 1$ $(j = 1, 2)$ in (2.1). The initial data in (2.2) is chosen as

$$\psi_1^0(\mathbf{x}) = \frac{x + iy}{\sqrt{\pi}} \exp\left(-\frac{x^2 + y^2}{2}\right), \quad \psi_2^0(\mathbf{x}) \equiv 0, \qquad \mathbf{x} \in \mathbb{R}^2. \tag{5.1}$$

The problem is solved numerically on a bounded computational domain $\Omega_{\mathbf{x}} = \{(x, y),\ r = \sqrt{x^2 + y^2} < R\}$ with $R = 12$ by the numerical method in the previous section and we choose mesh sizes $\Delta r = 0.005$, $\Delta\theta = \pi/128$ and time step $\Delta t = 0.0001$.

Figure 1 [**53**] shows the time evolution of density of each component for two sets of interaction parameters: (i) $\beta_{11} = \beta_{12} = \beta_{22} = 500$ (i.e. $a_{11} : a_{12} : a_{22} = 1 : 1 : 1$); (ii) $\beta_{11} = 500$, $\beta_{12} = 300$ and $\beta_{22} = 400$ (i.e. $a_{11} : a_{12} : a_{22} = 1 : 0.6 : 0.8$).

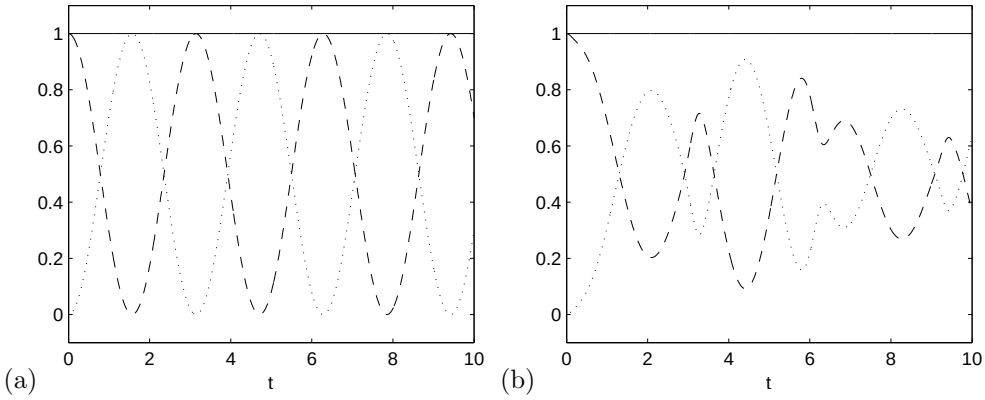

FIGURE 1. Time evolution of the densities $N_1(t) = \|\psi_1(\cdot, t)\|^2$ (dash line), $N_2(t) = \|\psi_2(\cdot, t)\|^2$ (dot line) and $N(t) = N_1(t) + N_2(t)$ (solid line) for two sets of interaction parameters: (a) $\beta_{11} = \beta_{12} = \beta_{22}$; (b) $\beta_{11} \neq \beta_{12} \neq \beta_{22}$.

From Fig. 1 [**53**], we can see that (i) the total density $N(t)$ is conserved in the discrete level for both cases; (ii) the densities of both components, i.e. $N_1(t)$ and $N_2(t)$, are periodic functions of period $T = 2\pi/\sqrt{4\lambda^2 + (\kappa_1 - \kappa_2)^2} = \pi$ when $\beta_{11} = \beta_{12} = \beta_{22}$ (cf. Fig. 1a); otherwise when $\beta_{11} \neq \beta_{12} \neq \beta_{22}$ they are periodic functions of period $T = \pi$ with a perturbation (cf. Fig. 1b), which confirms the analytical results in (3.33) and (3.34).

Example 2. Dynamics of vortex lattices [**53**], i.e. we $d = 2$, $\kappa_1 = \kappa_2 = 0$ and $\Omega = 0.9$ in (2.1). The initial data in (2.2) is taken as the stationary square vortex lattices [**53**], which are computed numerically by using the above parameters as well as $\lambda = 0$ and $\gamma_{x,j} = \gamma_{y,j} = 1$ $(j = 1, 2)$ in (2.1) [**?**]. The problem is solved numerically on a bounded computational domain $\Omega_{\mathbf{x}} = \{(x, y),\ r = \sqrt{x^2 + y^2} < R\}$ with $R = 12$ by the numerical method in the previous section and we choose mesh sizes $\Delta r = 0.005$, $\Delta\theta = \pi/128$ and time step $\Delta t = 0.0001$.

Figures 2 and 3 depict the contour plots of the wave functions $|\psi_1|^2$ and $|\psi_2|^2$ at different times for two cases: (i) adding an external driving field, i.e. at $t = 0$,

changing λ in (2.1) from 0 to 1, and (ii) changing the trapping frequencies, i.e. at $t = 0$, setting $\gamma_{x,1} = \gamma_{y,1} = 0.9$ and $\gamma_{x,2} = \gamma_{y,2} = 1.1$, respectively.

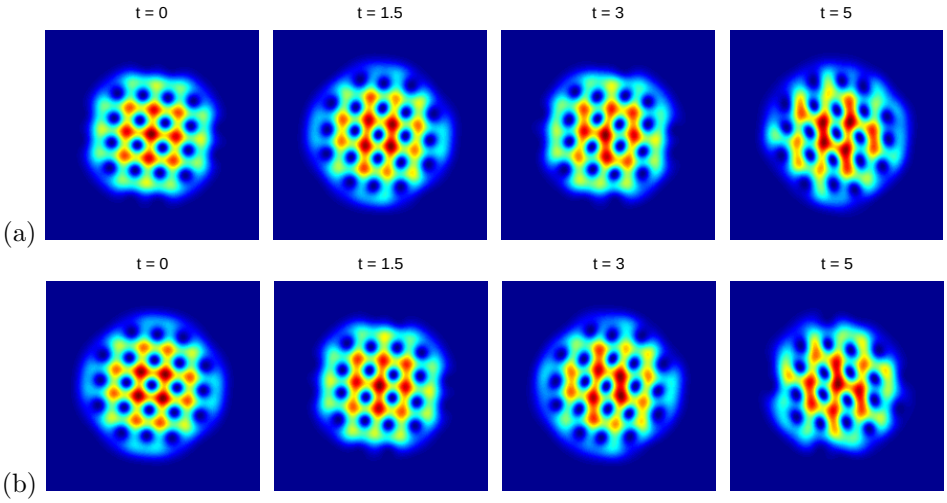

FIGURE 2. Contour plots of the wave functions $|\psi_1|^2$ (top row (a)) and $|\psi_2|^2$ (bottom row (b)) at different times for case (i).

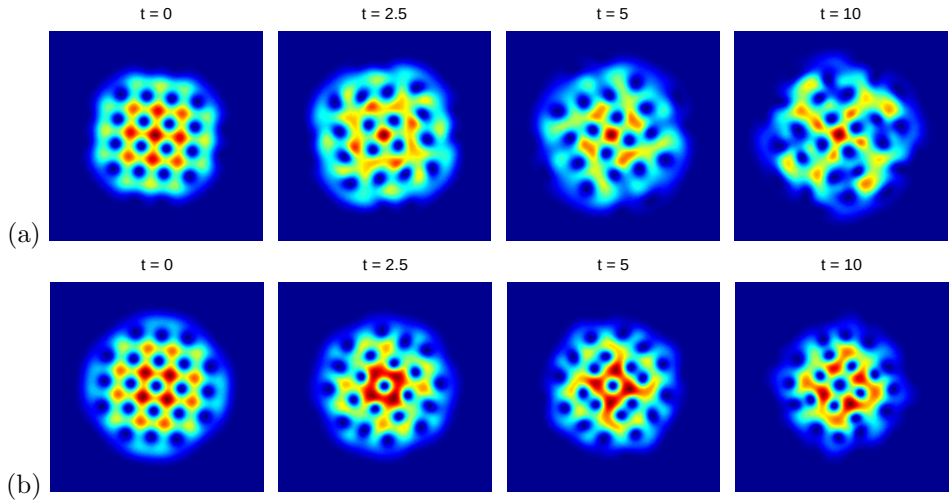

FIGURE 3. Contour plots of the wave functions $|\psi_1|^2$ (top row (a)) and $|\psi_2|^2$ (bottom row (b)) at different times for case (ii).

From Figs. 2 and 3 [**53**], we can see that initially there are two square lattices with about 16 and 21 quantized vortices in the first and second components, respectively (cf. Figs. 2&3 leftmost column). When we add an external driving field at $t = 0$, the two vortex lattices rotate due to the angular momentum term and shift their condensate shapes almost periodically due to the external driving field (cf.

Fig. 2). On the other hand, if we change the trapping frequencies at time $t = 0$, the two vortex lattices rotate again due to the angular momentum term but the condensate shape of each component keeps almost unchanged and the number of vortices in each lattice doesn't change during the dynamics (cf. Fig. 3). Of course, the lattice patterns are changed due to the inter-component interactions (cf. Figs. 2&3).

6. Conclusion

We reviewed some recent results on the dynamics of rotating two-component Bose-Einstein condensates (BEC) and their efficient and accurate computation. We began with the three-dimensional (3D) coupled Gross-Pitaevskii equations (GPEs) with an angular momentum rotation term and an external driving field, showed how to scale it into dimensionless form, reduce it to a 2D and 1D GPE in the limiting regime of strong anisotropic confinement and presented its semiclassical scaling and geometric optics. Analytical and numerical results for the dynamics of two-component BEC were reviewed. Finally, the analytical results and numerical methods for two-component BEC can be extended to spin-1 BEC [**10, 8, 51**].

Acknowledgment. I would like to thank my collaborators over the years for their help in appreciating the difficulties inherent to the mathematical analysis and numerical simulation for Bose-Einstein condensation: Peter A. Markowich, Dieter Jaksch, Qiang Du, Jie Shen, Hailiang Li, Yanzhi Zhang, Hanquan Wang, Weijun Tang, Fong Yin Lim, I-Liang Chern, Rada M. Weishäupl, Yunyi Ge and Ming-Huang Chai.

References

[1] J. R. Abo-Shaeer, C. Raman, J. M. Vogels and W. Ketterle, Observation of vortex lattices in Bose-Einstein condensates, Science, 292 (2001), pp. 476-479.
[2] M. H. Anderson, J. R. Ensher, M. R. Matthews, C. E. Wieman and E. A. Cornell, Observation of Bose-Einstein condensation in a dilute atomic vapor, Science, 269 (1995), pp. 198-201.
[3] J. R. Anglin and W. Ketterle, Bose-Einstein condensation of atomic gases, Nature, 416 (2002), pp. 211-218.
[4] W. Bao, Ground states and dynamics of multicomponent Bose-Einstein condensates, Multiscale Model. Simul., 2 (2004), pp. 210-236.
[5] W. Bao, Q. Du and Y. Zhang, Dynamics of rotating Bose-Einstein condensates and their efficient and accurate numerical computation, SIAM J. Appl. Math., 66 (2006), pp. 758-786.
[6] W. Bao, Y. Ge, D. Jaksch, P. A. Markowich and R. M. Weishaeupl, Convergence rate of dimension reduction in Bose-Einstein condensates, Comput. Phys. Comm., 177 (2007), pp. 832-850.
[7] W. Bao, D. Jaksch and P. A. Markowich, Numerical solution of the Gross-Pitaevskii equation for Bose-Einstein condensation, J. Comput. Phys., 187 (2003), pp. 318-342.
[8] W. Bao and F. Y. Lim, Computing ground states of spin-1 Bose-Einstein Condensates by the normalized gradient flow, SIAM J. Sci. Comput., to appear.
[9] W. Bao and J. Shen, A fourth-order time-splitting Laguerre-Hermite pseudo-spectral method for Bose-Einstein condensates, SIAM J. Sci. Comput., 26 (2005), pp. 2010-2028.
[10] W. Bao and H. Wang, An efficient and spectrally accurate numerical method for computing dynamics of rotating Bose-Einstein condensates, J. Comput. Phys., 217 (2006), pp. 612-626.
[11] W. Bao and H. Wang, A mass and magnetization conservative and energy diminishing numerical method for computing ground state of spin-1 Bose-Einstein condensates, SIAM J. Numer. Anal., 45 (2007), pp. 2177-2200.
[12] W. Bao, H. Wang and P. A. Markowich, Ground, symmetric and central vortex states in rotating Bose-Einstein condensates, Comm. Math. Sci., 3 (2005), pp. 57-88.

[13] W. Bao and Y. Zhang, Dynamics of the ground state and central vortex states in Bose-Einstein condensation, Math. Mod. Meth. Appl. Sci., 15 (2005), pp. 1863-1896.
[14] C. C. Bradley, C. A. Sackett and R. G. Hulet, Bose-Einstein condensation of lithium: observation of limited condensate number, Phys. Rev. Lett., 78 (1997), pp. 985-989.
[15] R. Carles, WKB analysis for nonlinear Schrödinger equations with potential, Comm. Math. Phys., 269 (2007), pp. 195-221.
[16] S. -M. Chang, W. -W. Lin and S. -F., Shieh, Gauss-Seidel-type methods for energy states of a multi-component Bose-Einstein condensate, J. Comput. Phys., 202 (2005), pp. 367-390.
[17] S. M. Chang, C. S. Lin, T. C. Lin and W. W. Lin, Segregated nodal domains of two-dimensional multispecies Bose-Einstein condensates, Physica D, 196 (2004), pp. 341-361.
[18] S. T. Chui, V. N. Ryzhov and E. E. Tareyeva, Phase separation and vortex states in the binary mixture of Bose-Einstein condensates, J. Exper. Thect. Phys., 91 (2000), pp. 1183-1189.
[19] K. B. Davis, M. -O. Mewes, M. R. Andrews, N. J. van Druten, D. S. Durfee, D. M. Kurn and W. Ketterle, Bose-Einstein condensation in a gas of sodium atoms, Phys. Rev. Lett., 75 (1995), pp. 3969-3973.
[20] B. D. Esry, C. H. Greene, J. P. Burke, Jr. and J. L. Bohn, Hartree-Fock theory for double condensates, Phys. Rev. Lett., 78 (1997), pp. 3594-3597.
[21] J. J. Garcia-Ripoll and V. M. Perez-Garcia, Stable and unstable vortices in multicomponent Bose-Einstein condensates, Phys. Rev. Lett., 84 (2000), pp. 4264-4267.
[22] J. J. Garcia-Ripoll and V. M. Perez-Garcia, Split vortices in optically coupled Bose-Einstein condensates, Phys. Rev. A, 66(2002), pp. 021602.
[23] J. J. Garcia-Ripoll and V. M. Perez-Garcia and V. Vekslerchik, Construction of exact solutions by spatial translations in inhomogeneous nonlinear Schrödinger equations, Phys. Rev. E, 64 (2001), pp. 056602.
[24] I. Gasser and P.A. Markowich, Quantum hydrodynamics, Winger transforms and the classical limit, Assymptot. Anal., 14 (1997), pp. 97-116.
[25] P. Gerard, P.A. Markowich, N.J. Mauser and F. Poupaud, Homogenization limits and Wigner transforms, Comm. Pure Appl. Math., 50 (1997), pp. 321-377.
[26] E. V. Goldstein, M. G. Moore, H. Pu and P. Meystre, Eliminating the mean-field shift in two-component Bose-Einstein condensates, Phys. Rev. Lett., 85 (2000), pp. 5030-5033.
[27] E. Grenier, Semiclassical limit of the nonlinear Schrödinger equation in small time, Proc. Amer. Math. Soc., 126 (1998), pp. 523-530.
[28] D. S. Hall, M. R. Matthews, J. R. Ensher, C. E. Wieman and E. A. Cornell, Dynamics of component separation in a binary mixture of Bose-Einstein condensates, Phys. Rev. Lett., 81 (1998), pp. 1539-1542.
[29] T. -L. Ho and V. B. Shenoy, Binary mixtures of Bose condensates of alkali atoms, Phys. Rev. Lett., 77 (1996), pp. 3276-3279.
[30] D. Jaksch, S. A. Gardiner, K. Schulze, J. I. Cirac and P. Zoller, Uniting Bose-Einstein condensates in optical resonators, Phys. Rev. Lett., 86 (2001), pp. 4733-4736.
[31] D. M. Jezek, P. Capuzzi and H. M. Cataldo, Structure of vortices in two-component Bose-Einstein condensates, Phys. Rev. A, 64 (2001), pp. 023605.
[32] K. Kasamatsu, M. Tsubota and M. Ueda, Vortex phase diagram in rotating two-component Bose-Einstein condensates, Phys. Rev. Lett., 91 (2003), pp. 150406.
[33] K. Kasamatsu, M. Tsubota and M. Ueda, Vortices in multicomponent Bose-Einstein condensates, Inter. J. Modern Phys. B, 19 (2005), pp. 1835-1904.
[34] M. -C. Lai, W. -W. Lin, and W. Wang, A fast spectral/difference method without pole conditions for Poisson-type equations in cylindrical and spherical geometries, IMA J. Numer. Anal., 22 (2002), pp. 537-548.
[35] C. K. Law, H. Pu, N. P. Bigelow and J. H. Eberly, "Stability signature" in two-species dilute Bose-Einstein condensates, Phys. Rev. Lett., 79 (1997), pp. 3105-3108.
[36] E. H. Lieb and R. Seiringer, Derivation of the Gross-Pitaevskii equation for rotating Bose gases, Comm. Math. Phys., 264 (2006), pp. 505-537.
[37] E. H. Lieb and J. P. Solovej, Ground state energy of the two-component charged Bose gas, Comm. Math. Phys., 252 (2004), pp. 485-534.
[38] T. -C. Lin and J. Wei, Ground state of N coupled nonlinear Schrödinger Equations in $\mathbb{R}^n$, $n \leq 3$, Comm. Math. Phys., 255 (2005), pp. 629-653.
[39] T. -C. Lin and J. Wei, Spikes in two-component systems of nonlinear Schrödinger equations with trapping potentials, J. Diff. Equ., 229 (2006), pp. 538-569.

[40] K. W. Madison, F. Chevy, W. Wohlleben and J. Dalibard, Vortex formation in a stirred Bose-Einstein condensate, Phys. Rev. Lett., 84 (2000), pp. 806-809.
[41] A. Minguzzi, S. Succi, F. Toschi, M. P. Tosi and P. Vignolo, Numerical methods for atomic quantum gases with applications to Bose-Einstein condensates and to ultracold fermions, Phys. Rep., 395 (2004), pp. 223-355.
[42] E. J. Mueller and T. -L. Ho, Two-component Bose-Einstein condensates with a large number of vortices, Phys. Rev. Lett., 88 (2002), pp. 180403.
[43] C. J. Myatt, E. A. Burt, R. W. Ghrist, E. A. Cornell and C. E. Wieman, Production of two overlapping Bose-Einstein condensates by sympathetic cooling, Phys. Rev. Lett., 78 (1997), pp. 586-589.
[44] L. P. Pitaevskii and S. Stringari, Bose-Einstein condensation, Clarendon Press, 2003.
[45] H. Pu and N. P. Bigelow, Properties of two-species Bose condensates, Phys. Rev. Lett., 80 (1998), pp. 1130-1133.
[46] F. Riboli and M. Modugno, Topology of the ground state of two interacting Bose-Einstein condensates, Phys. Rev. A, 65 (2002), pp. 063614.
[47] B. I. Schneider and D. L. Feder, Numerical approach to the ground and excited states of a Bose-Einstein condensed gas confined in a completely anisotropic trap, Phys. Rev. A, 59 (1999), pp. 2232-2242.
[48] D. M. Stamper-Kurn, M. R. Andrews, A. P. Chikkatur, S. Inouye, H. J. Miesner, J. Stenger and W. Ketterle, Optical confinement of a Bose-Einstein condensate, Phys. Rev. Lett., 80 (1998), pp. 2027-2030.
[49] G. Strang, On the construction and comparison of difference schemes, SIAM J. Numer. Anal., 5 (1968), pp. 505-517.
[50] H. Wang, A time-splitting spectral method for coupled Gross-Pitaevskii equations with applications to rotating Bose-Einstein condensates, J. Comput. Appl. Math., 205 (2007), pp. 88-104.
[51] H. Wang, A time-splitting spectral method for computing dynamics of spinor F=1 Bose-Einstein condensates, Int. J. Computer Math., 84 (2007), pp. 925-944.
[52] Y. Zhang and W. Bao, Dynamics of the center of mass in rotating Bose-Einstein condensates, Appl. Numer. Math., 57 (2007), pp. 697-709.
[53] Y. Zhang, W. Bao and H.-L. Li, Dynamics of rotating two-component Bose-Einstein condensates and its efficient computation, Physica D, 234 (2007), pp. 49-69.

Department of Mathematics and Center for Computational Science and Engineering, National University of Singapore, Singapore 11743
E-mail address: bao@math.nus.edu.sg; URL: http://www.math.nus.edu.sg/~bao/